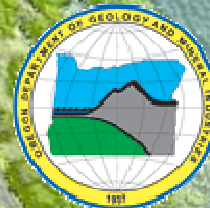


LIDAR REMOTE SENSING DATA COLLECTION DEPARTMENT OF GEOLOGY AND MINERAL INDUSTRIES SOUTHWESTERN OREGON

JANUARY 30, 2009

Submitted to:

Department of Geology and Mineral Industries
800 NE Oregon Street, Suite 965
Portland, OR 97232



Submitted by:

Watershed Sciences
529 SW Third Ave, Suite 300
Portland, OR 97204

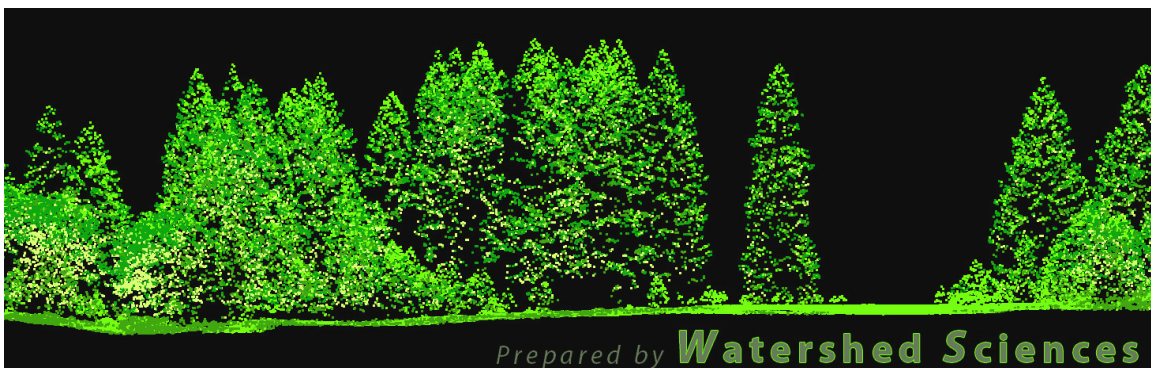


LIDAR REMOTE SENSING DATA COLLECTION:

DOGAMI, SOUTHERN OREGON COAST STUDY AREA

TABLE OF CONTENTS

1. Overview	1
1.1 Department of Geology and Mineral Industries Study Area (South Coast) ..	1
1.2 Area Delivered to Date	2
1.3 Accuracy and Resolution	4
1.4 Data Format, Projection, and Units	4
2. Acquisition	5
2.1 Airborne Survey - Instrumentation and Methods	5
2.2 Ground Survey - Instrumentation and Methods	7
2.3 Real-Time Kinematic Survey Results	9
3. LiDAR Data Processing	13
3.1 Applications and Work Flow Overview	13
3.2 Aircraft Kinematic GPS and IMU Data	13
3.3 Laser Point Processing	14
4. LiDAR Accuracy and Resolution	15
4.1 Laser Point Accuracy	15
4.1.1 Relative Accuracy	15
4.1.2 Absolute Accuracy	19
4.2 Data Density/Resolution	21
4.2.1 First Return Laser Pulses per Square Foot	21
4.2.2 Classified Ground Points per Square Foot	23
4.3 Data Density/Resolution per Delivery	25
4.3.1 Delivery 1	25
4.3.2 Delivery 2	26
4.3.3 Delivery 3	28
4.3.4 Delivery 4	29
5. Deliverables	31
5.1 Point Data (per 0.75' USGS Quad)	32
5.2 Vector Data	32
5.3 Raster Data	32
5.4 Data Report	32
5.5 Datum and Projection	32
6. Selected Imagery	33
7. Glossary	42
8. Citations	43

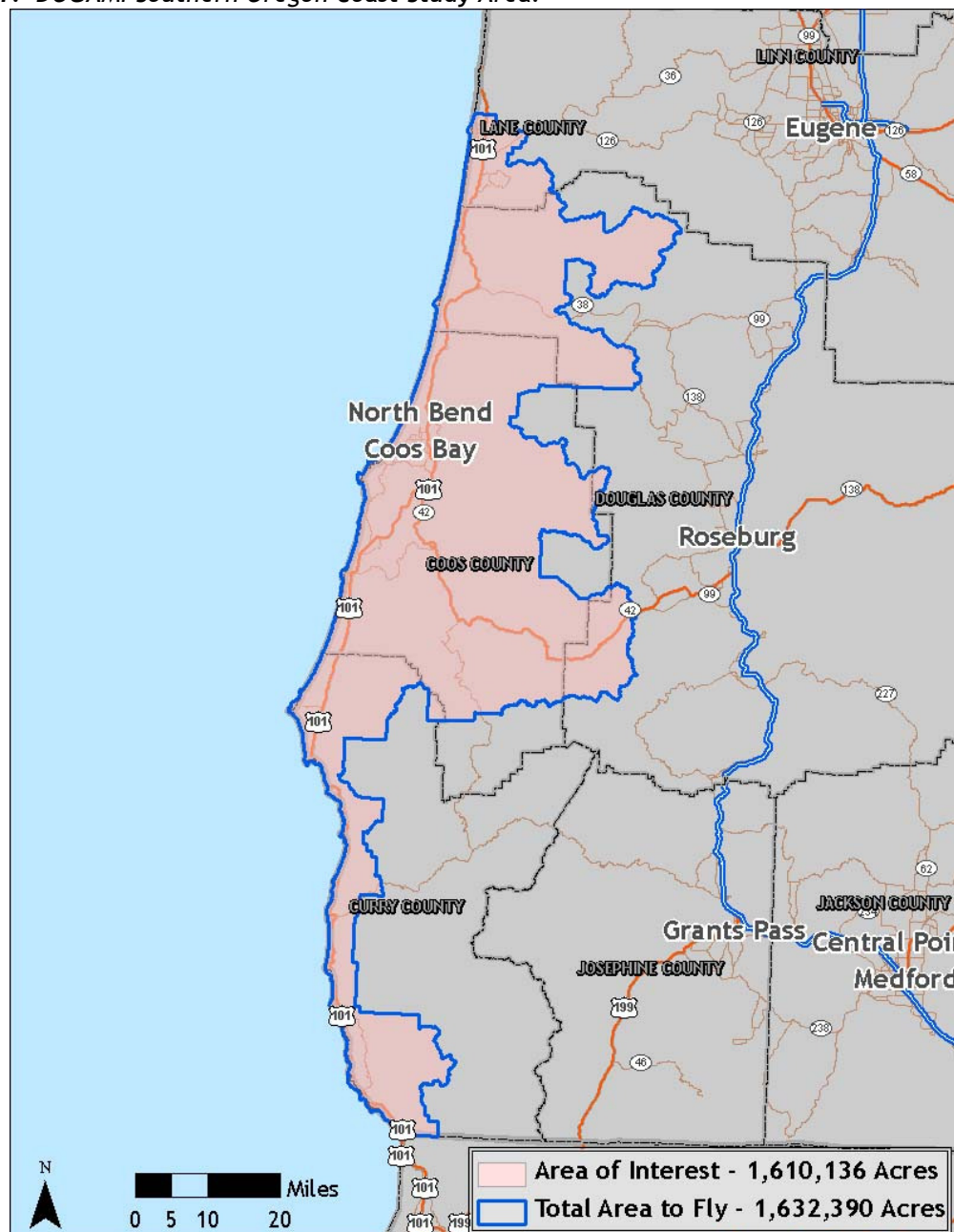


1. Overview

1.1 Department of Geology and Mineral Industries Study Area (South Coast)

Watershed Sciences, Inc. (WS) is collecting Light Detection and Ranging (LiDAR) data for the Department of Geology and Mineral Industries (DOGAMI). The Area of Interest (AOI) covers portions of four counties in southwest Oregon. The requested LiDAR area totals ~1,610,136 acres; the map below shows the Total Area to be Flown (TAF), covering ~1,632,390 acres. The TAF acreage is greater than the original AOI acreage due to buffering and flight planning optimization. The DOGAMI study area will be acquired and processed as logistical constraints and weather allow. This report will be amended to reflect new data and cumulative statistics for the overall LiDAR survey.

Figure 1.1. DOGAMI Southern Oregon Coast Study Area.



1.2 Area Delivered to Date

Total delivered acreage to date is detailed below.

DOGAMI Southern Oregon Coast				
	Delivery Date	Acquisition Date	AOI Acres	TAF Acres
Delivery 1	September 3, 2008	May 3 - June 26, 2008	46,568	47,798
Delivery 2	October 2, 2008	May 3 - June 26, 2008	86,505	88,789
Delivery 3	October 16, 2008	May 3 - June 26, 2008	68,913	71,791
Delivery 4	November 21, 2008	June 12 - June 29, 2008	111,851	113,638
Delivery 5	January 19, 2009	June 12 - June 29, 2008	113,350	113,794
		Total	427,187	435,810

Figure 1.2. DOGAMI southern Oregon coast study area, illustrating the delivered portion of the TAF.

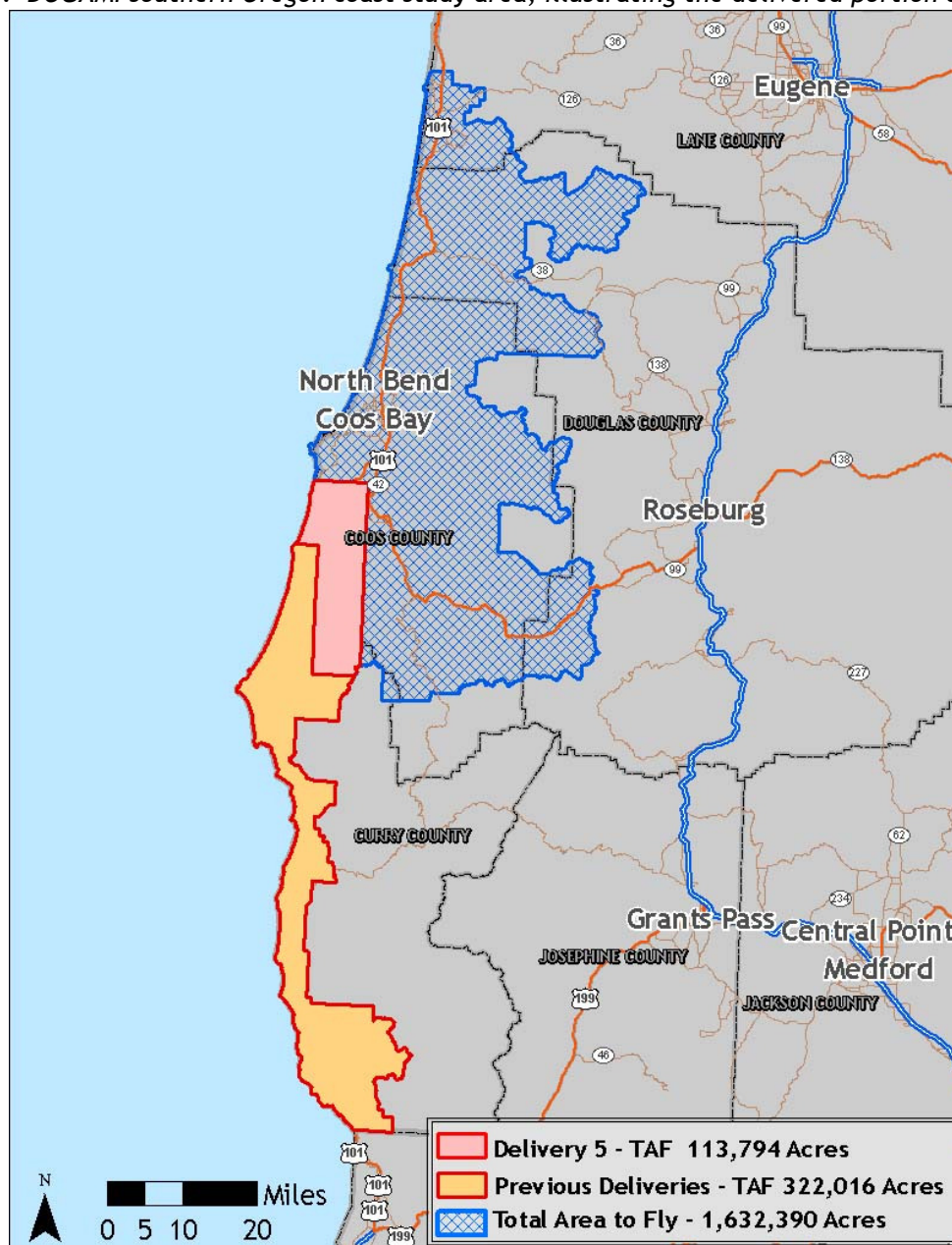
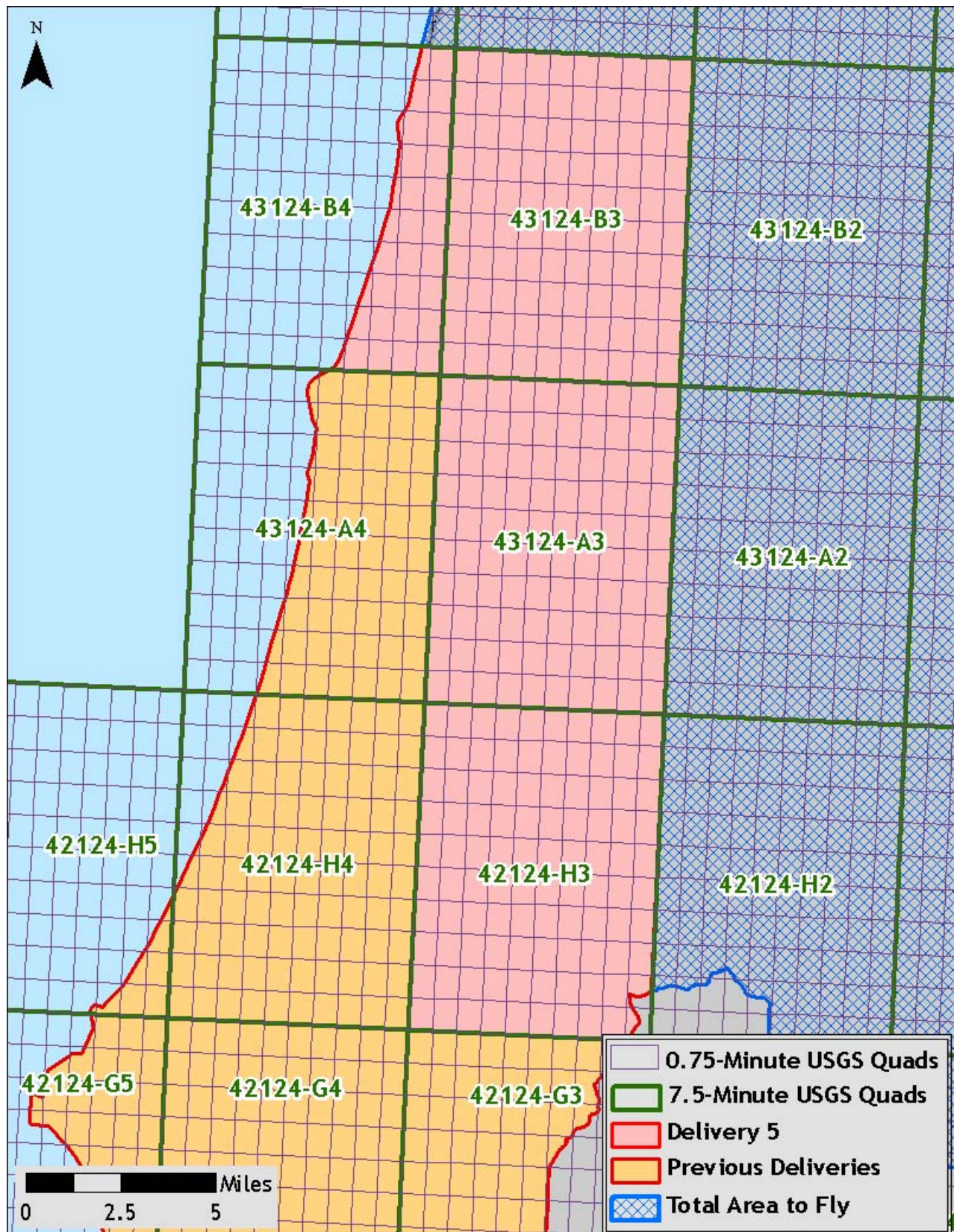


Figure 1.3. DOGAMI study areas, illustrating the delivered 7.5 and 0.75-minute USGS quads.



1.3 Accuracy and Resolution

Real-time kinematic (RTK) surveys were conducted in multiple locations throughout the study area for quality assurance purposes. The accuracy of the LiDAR data is described as standard deviations of divergence ($\sigma \sim \sigma$) from RTK ground survey points and root mean square error (RMSE) which considers bias (upward or downward). These statistics are calculated cumulatively. For the DOGAMI study area, the data have the following accuracy statistics:

- RMSE of 0.15 feet
- 1-sigma absolute deviation of 0.15 feet
- 2-sigma absolute deviation of 0.34 feet

Data resolution specifications are for ≥ 8 pts per square meter. **Total pulse density for the data delivered to date is 8.50 points per square meter (0.79 points per square foot).**

1.4 Data Format, Projection, and Units

Deliverables include point data in *.las v 1.1 format, 3-foot resolution bare ground model ESRI GRID, 3-foot resolution above ground surface ESRI GRID, 1.5-foot resolution intensity images in GeoTIFF format, 3-foot resolution ground density rasters, shapefiles of study area and ground control points, and data report.

DOGAMI data are delivered in Oregon Lambert (NAD 83), with horizontal and vertical units in International Feet, in the NAD83 HARN/NAVD88 datum (Geoid 03).

2. Acquisition

2.1 Airborne Survey - Instrumentation and Methods

The LiDAR survey utilized a Leica ALS50 Phase II mounted in Cessna Caravan 208B. The system was set to acquire $\geq 105,000$ laser pulses per second (i.e., 105 kHz pulse rate) and flown at 900 meters above ground level (AGL), capturing a scan angle of $\pm 14^\circ$ from nadir¹. These settings are developed to yield points with an average native density of ≥ 8 points per square meter over terrestrial surfaces. The native pulse density is the number of pulses emitted by the LiDAR system. Some types of surfaces (i.e., dense vegetation or water) may return fewer pulses than the laser originally emitted. Therefore, the delivered density can be less than the native density and lightly variable according to distributions of terrain, land cover and water bodies.



The Cessna Caravan is a powerful, stable platform, which is ideal for the often remote and mountainous terrain found in the Pacific Northwest. The Leica ALS50 sensor head installed in the Caravan is shown on the right.

The completed areas were surveyed with opposing flight line side-lap of $\geq 50\%$ ($\geq 100\%$ overlap) to reduce laser shadowing and increase surface laser painting. The system allows up to four range measurements per pulse, and all discernable laser returns were processed for the output dataset.

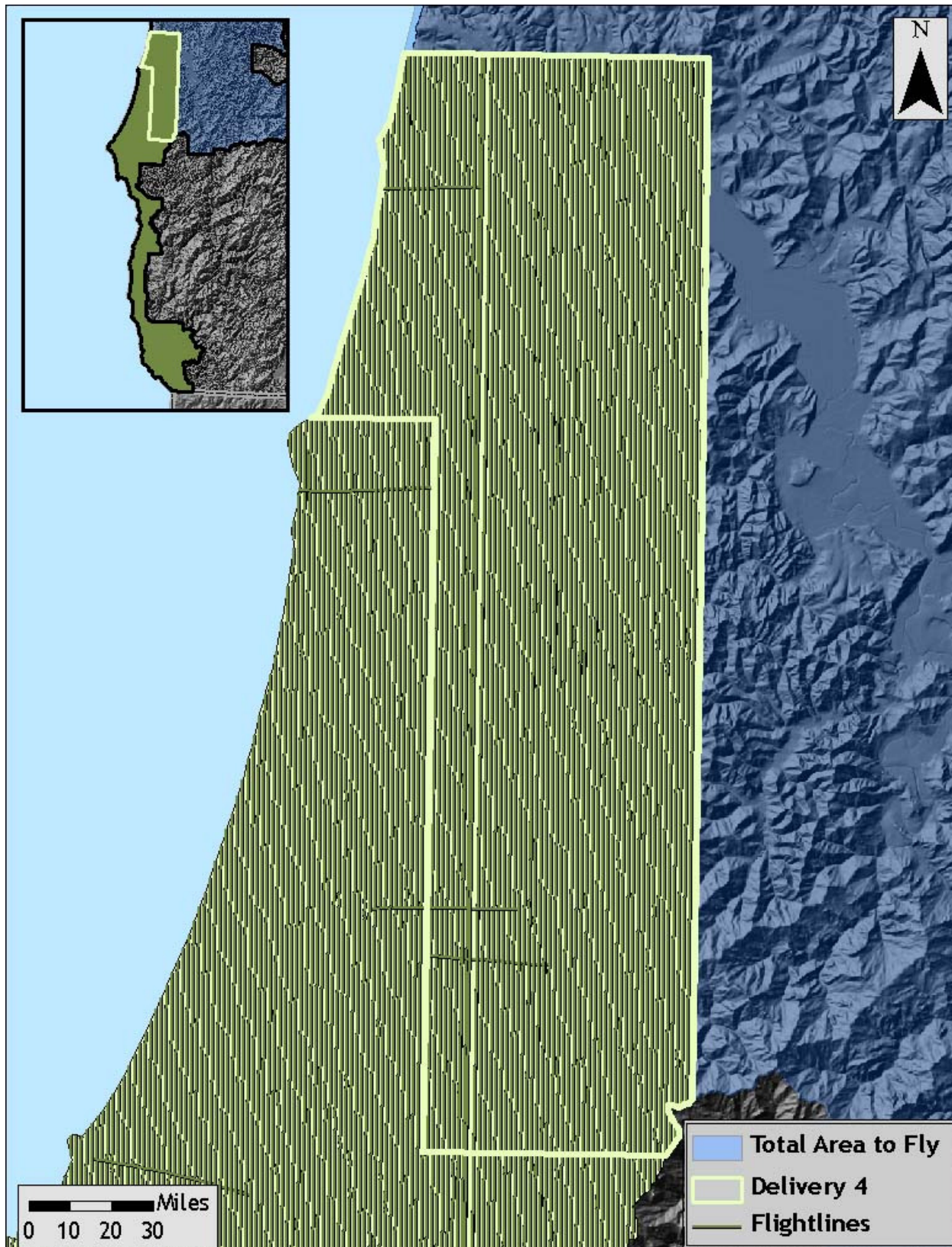
To solve for laser point position, it is vital to have an accurate description of aircraft position and attitude. Aircraft position is described as x, y and z and measured twice per second (2 Hz) by an onboard differential GPS unit. Aircraft attitude is measured 200 times per second (200 Hz) as pitch, roll and yaw (heading) from an onboard inertial measurement unit (IMU). Table 2.1 provides the survey specifications and the flightline trajectories are shown in Figure 2.1.

Table 2.1 LiDAR Survey Specifications

Sensor	Leica ALS50 Phase II
Survey Altitude (AGL)	900 m
Pulse Rate	> 105 kHz
Pulse Mode	Single
Mirror Scan Rate	52.2 Hz
Field of View	28° ($\pm 14^\circ$ from nadir)
Roll Compensated	Up to 20°
Overlap	100% (50% Side-lap)

¹ Nadir refers to the perpendicular vector to the ground directly below the aircraft. Nadir is commonly used to measure the angle from the vector and is referred to a “degrees from nadir”.

Figure 2.1. Actual flightlines for data delivered to date in the southern Oregon coast study area.



2.2 Ground Survey - Instrumentation and Methods

During the LiDAR survey of the study area, a static (1 Hz recording frequency) ground survey was conducted over monuments with known coordinates. Coordinates are provided in **Table 2.2** below and shown in **Figure 2.2**. After the airborne survey, the static GPS data are processed using triangulation with CORS stations and checked against the Online Positioning User Service (OPUS²) to quantify daily variance. Multiple sessions are processed over the same monument to confirm antenna height measurements and reported position accuracy.

Whenever possible multiple sessions were observed at base station locations. All sessions were statistically compared to each other in order to ensure accurate base station coordinates and elimination of systematic errors that might otherwise be incorporated into the data. At least 3 observations and a standard deviation of 1cm or less among observations in the Northing, Easting, and Ellipsoidal fields were required for a base station location to be used for LiDAR flight processing purposes. In some cases the 3 session minimum was not possible for real-time kinematic (RTK) base station locations. For these locations a minimum 6 hour first session was taken and was then followed by a half-hour short session that was used to ensure that no errors occurred during the initial occupation.

Table 2.2. Base Station Surveyed Coordinates, (NAD83/NAVD88, OPUS corrected) used for post-processing of the aircraft GPS data and the ground RTK for the DOGAMI AOIs.

	Datum NAD83(HARN)		GRS80
Base Station ID	Latitude (North)	Longitude (West)	Ellipsoid Height (m)
OLCJN1	42 08 30.08496	124 12 49.11911	428.475
OLCJN2	42 08 27.95822	124 12 49.29884	427.870
OLCJN3	42 03 04.54697	124 17 30.17996	1.811
OLCJN4	42 03 50.25255	124 12 46.39603	31.933
OLCJN5	42 28 05.44507	124 20 46.24558	-21.890
OLCJN6	42 25 33.04097	124 25 35.72884	-19.346
OLCJN7	42 48 31.65550	124 29 21.62711	33.225
OLCJN8	43 09 26.13789	124 22 44.20041	-19.734
OLCJN9	42 47 10.43094	124 28 52.40738	-13.568
OLCPWH1	42 19 43.74040	124 25 33.76978	177.778
OLCPWH2	42 32 11.15305	124 23 59.59628	-13.175
OLCPWH3	42 27 48.10893	124 21 45.53382	-15.340
OLCPWH4	42 16 31.44293	124 24 15.39346	-21.678
OLCPWH5	42 48 26.82761	124 20 09.43708	68.264
OLCPWH6	43 07 56.53594	124 21 10.15905	-22.854
OLCPWH7	43 15 44.29178	123 49 12.34815	32.003
OLCBTK1	42 07 32.49487	124 18 37.00074	295.173
OLCBTK2	42 04 08.31008	124 18 52.63704	-16.064
OLCBTK3	42 08 39.24373	124 21 22.62505	-6.578
OLCBTK4	42 02 44.62353	124 16 04.64324	-21.946
NGS_PID_OA07	43 5 54.88105	124 24 55.03463	-0.860
DH7020	43 5 11.08316	124 24 26.18403	7.977

² Online Positioning User Service (OPUS) is run by the National Geodetic Survey to process corrected monument positions.

A map of the OLC region showing the locations of base stations. The map includes a legend in the top right corner with two entries: a red triangle symbol for 'Base Stations' and a yellow rectangle with a red border for 'Data delivered to date'. The map shows a yellow-shaded area representing the OLC region, with a red outline. Base stations are marked with red triangles and labeled with codes: OLCJN8, OLCJN9, OLCJN7, OLCJN6, OLCJN5, OLCJN4, OLCJN3, OLCJN2, OLCJN1, OLCJN0, OLCJN10, OLCJN11, OLCJN12, OLCJN13, OLCJN14, OLCJN15, OLCJN16, OLCJN17, OLCJN18, OLCJN19, OLCJN20, OLCJN21, OLCJN22, OLCJN23, OLCJN24, OLCJN25, OLCJN26, OLCJN27, OLCJN28, OLCJN29, OLCJN30, OLCJN31, OLCJN32, OLCJN33, OLCJN34, OLCJN35, OLCJN36, OLCJN37, OLCJN38, OLCJN39, OLCJN40, OLCJN41, OLCJN42, OLCJN43, OLCJN44, OLCJN45, OLCJN46, OLCJN47, OLCJN48, OLCJN49, OLCJN50, OLCJN51, OLCJN52, OLCJN53, OLCJN54, OLCJN55, OLCJN56, OLCJN57, OLCJN58, OLCJN59, OLCJN60, OLCJN61, OLCJN62, OLCJN63, OLCJN64, OLCJN65, OLCJN66, OLCJN67, OLCJN68, OLCJN69, OLCJN70, OLCJN71, OLCJN72, OLCJN73, OLCJN74, OLCJN75, OLCJN76, OLCJN77, OLCJN78, OLCJN79, OLCJN80, OLCJN81, OLCJN82, OLCJN83, OLCJN84, OLCJN85, OLCJN86, OLCJN87, OLCJN88, OLCJN89, OLCJN90, OLCJN91, OLCJN92, OLCJN93, OLCJN94, OLCJN95, OLCJN96, OLCJN97, OLCJN98, OLCJN99, OLCJN100, OLCJN101, OLCJN102, OLCJN103, OLCJN104, OLCJN105, OLCJN106, OLCJN107, OLCJN108, OLCJN109, OLCJN110, OLCJN111, OLCJN112, OLCJN113, OLCJN114, OLCJN115, OLCJN116, OLCJN117, OLCJN118, OLCJN119, OLCJN120, OLCJN121, OLCJN122, OLCJN123, OLCJN124, OLCJN125, OLCJN126, OLCJN127, OLCJN128, OLCJN129, OLCJN130, OLCJN131, OLCJN132, OLCJN133, OLCJN134, OLCJN135, OLCJN136, OLCJN137, OLCJN138, OLCJN139, OLCJN140, OLCJN141, OLCJN142, OLCJN143, OLCJN144, OLCJN145, OLCJN146, OLCJN147, OLCJN148, OLCJN149, OLCJN150, OLCJN151, OLCJN152, OLCJN153, OLCJN154, OLCJN155, OLCJN156, OLCJN157, OLCJN158, OLCJN159, OLCJN160, OLCJN161, OLCJN162, OLCJN163, OLCJN164, OLCJN165, OLCJN166, OLCJN167, OLCJN168, OLCJN169, OLCJN170, OLCJN171, OLCJN172, OLCJN173, OLCJN174, OLCJN175, OLCJN176, OLCJN177, OLCJN178, OLCJN179, OLCJN180, OLCJN181, OLCJN182, OLCJN183, OLCJN184, OLCJN185, OLCJN186, OLCJN187, OLCJN188, OLCJN189, OLCJN190, OLCJN191, OLCJN192, OLCJN193, OLCJN194, OLCJN195, OLCJN196, OLCJN197, OLCJN198, OLCJN199, OLCJN200, OLCJN201, OLCJN202, OLCJN203, OLCJN204, OLCJN205, OLCJN206, OLCJN207, OLCJN208, OLCJN209, OLCJN210, OLCJN211, OLCJN212, OLCJN213, OLCJN214, OLCJN215, OLCJN216, OLCJN217, OLCJN218, OLCJN219, OLCJN220, OLCJN221, OLCJN222, OLCJN223, OLCJN224, OLCJN225, OLCJN226, OLCJN227, OLCJN228, OLCJN229, OLCJN230, OLCJN231, OLCJN232, OLCJN233, OLCJN234, OLCJN235, OLCJN236, OLCJN237, OLCJN238, OLCJN239, OLCJN240, OLCJN241, OLCJN242, OLCJN243, OLCJN244, OLCJN245, OLCJN246, OLCJN247, OLCJN248, OLCJN249, OLCJN250, OLCJN251, OLCJN252, OLCJN253, OLCJN254, OLCJN255, OLCJN256, OLCJN257, OLCJN258, OLCJN259, OLCJN260, OLCJN261, OLCJN262, OLCJN263, OLCJN264, OLCJN265, OLCJN266, OLCJN267, OLCJN268, OLCJN269, OLCJN270, OLCJN271, OLCJN272, OLCJN273, OLCJN274, OLCJN275, OLCJN276, OLCJN277, OLCJN278, OLCJN279, OLCJN280, OLCJN281, OLCJN282, OLCJN283, OLCJN284, OLCJN285, OLCJN286, OLCJN287, OLCJN288, OLCJN289, OLCJN290, OLCJN291, OLCJN292, OLCJN293, OLCJN294, OLCJN295, OLCJN296, OLCJN297, OLCJN298, OLCJN299, OLCJN300, OLCJN301, OLCJN302, OLCJN303, OLCJN304, OLCJN305, OLCJN306, OLCJN307, OLCJN308, OLCJN309, OLCJN310, OLCJN311, OLCJN312, OLCJN313, OLCJN314, OLCJN315, OLCJN316, OLCJN317, OLCJN318, OLCJN319, OLCJN320, OLCJN321, OLCJN322, OLCJN323, OLCJN324, OLCJN325, OLCJN326, OLCJN327, OLCJN328, OLCJN329, OLCJN330, OLCJN331, OLCJN332, OLCJN333, OLCJN334, OLCJN335, OLCJN336, OLCJN337, OLCJN338, OLCJN339, OLCJN340, OLCJN341, OLCJN342, OLCJN343, OLCJN344, OLCJN345, OLCJN346, OLCJN347, OLCJN348, OLCJN349, OLCJN350, OLCJN351, OLCJN352, OLCJN353, OLCJN354, OLCJN355, OLCJN356, OLCJN357, OLCJN358, OLCJN359, OLCJN360, OLCJN361, OLCJN362, OLCJN363, OLCJN364, OLCJN365, OLCJN366, OLCJN367, OLCJN368, OLCJN369, OLCJN370, OLCJN371, OLCJN372, OLCJN373, OLCJN374, OLCJN375, OLCJN376, OLCJN377, OLCJN378, OLCJN379, OLCJN380, OLCJN381, OLCJN382, OLCJN383, OLCJN384, OLCJN385, OLCJN386, OLCJN387, OLCJN388, OLCJN389, OLCJN390, OLCJN391, OLCJN392, OLCJN393, OLCJN394, OLCJN395, OLCJN396, OLCJN397, OLCJN398, OLCJN399, OLCJN400, OLCJN401, OLCJN402, OLCJN403, OLCJN404, OLCJN405, OLCJN406, OLCJN407, OLCJN408, OLCJN409, OLCJN410, OLCJN411, OLCJN412, OLCJN413, OLCJN414, OLCJN415, OLCJN416, OLCJN417, OLCJN418, OLCJN419, OLCJN420, OLCJN421, OLCJN422, OLCJN423, OLCJN424, OLCJN425, OLCJN426, OLCJN427, OLCJN428, OLCJN429, OLCJN430, OLCJN431, OLCJN432, OLCJN433, OLCJN434, OLCJN435, OLCJN436, OLCJN437, OLCJN438, OLCJN439, OLCJN440, OLCJN441, OLCJN442, OLCJN443, OLCJN444, OLCJN445, OLCJN446, OLCJN447, OLCJN448, OLCJN449, OLCJN450, OLCJN451, OLCJN452, OLCJN453, OLCJN454, OLCJN455, OLCJN456, OLCJN457, OLCJN458, OLCJN459, OLCJN460, OLCJN461, OLCJN462, OLCJN463, OLCJN464, OLCJN465, OLCJN466, OLCJN467, OLCJN468, OLCJN469, OLCJN470, OLCJN471, OLCJN472, OLCJN473, OLCJN474, OLCJN475, OLCJN476, OLCJN477, OLCJN478, OLCJN479, OLCJN480, OLCJN481, OLCJN482, OLCJN483, OLCJN484, OLCJN485, OLCJN486, OLCJN487, OLCJN488, OLCJN489, OLCJN490, OLCJN491, OLCJN492, OLCJN493, OLCJN494, OLCJN495, OLCJN496, OLCJN497, OLCJN498, OLCJN499, OLCJN500, OLCJN501, OLCJN502, OLCJN503, OLCJN504, OLCJN505, OLCJN506, OLCJN507, OLCJN508, OLCJN509, OLCJN510, OLCJN511, OLCJN512

2.3 Real-Time Kinematic Survey Results

Multiple DGPS units are used for the ground RTK portion of the survey. To collect accurate ground surveyed points, a GPS base unit is set up over monuments to broadcast a kinematic correction to a roving GPS unit. The ground crew uses a roving unit to receive radio-relayed kinematic corrected positions from the base unit. The RTK survey allows precise location measurement ($\sigma \leq 1.5 \text{ cm} \sim 0.6 \text{ in}$). For data delivered to date, 12,377 RTK points were collected in the study area. **Figures 2.3-2.5** show detailed views of RTK point locations.



Trimble GPS survey equipment configured for collecting RTK data.

Figure 2.3. RTK point locations in the study area; images are NAIP Orthoimages.

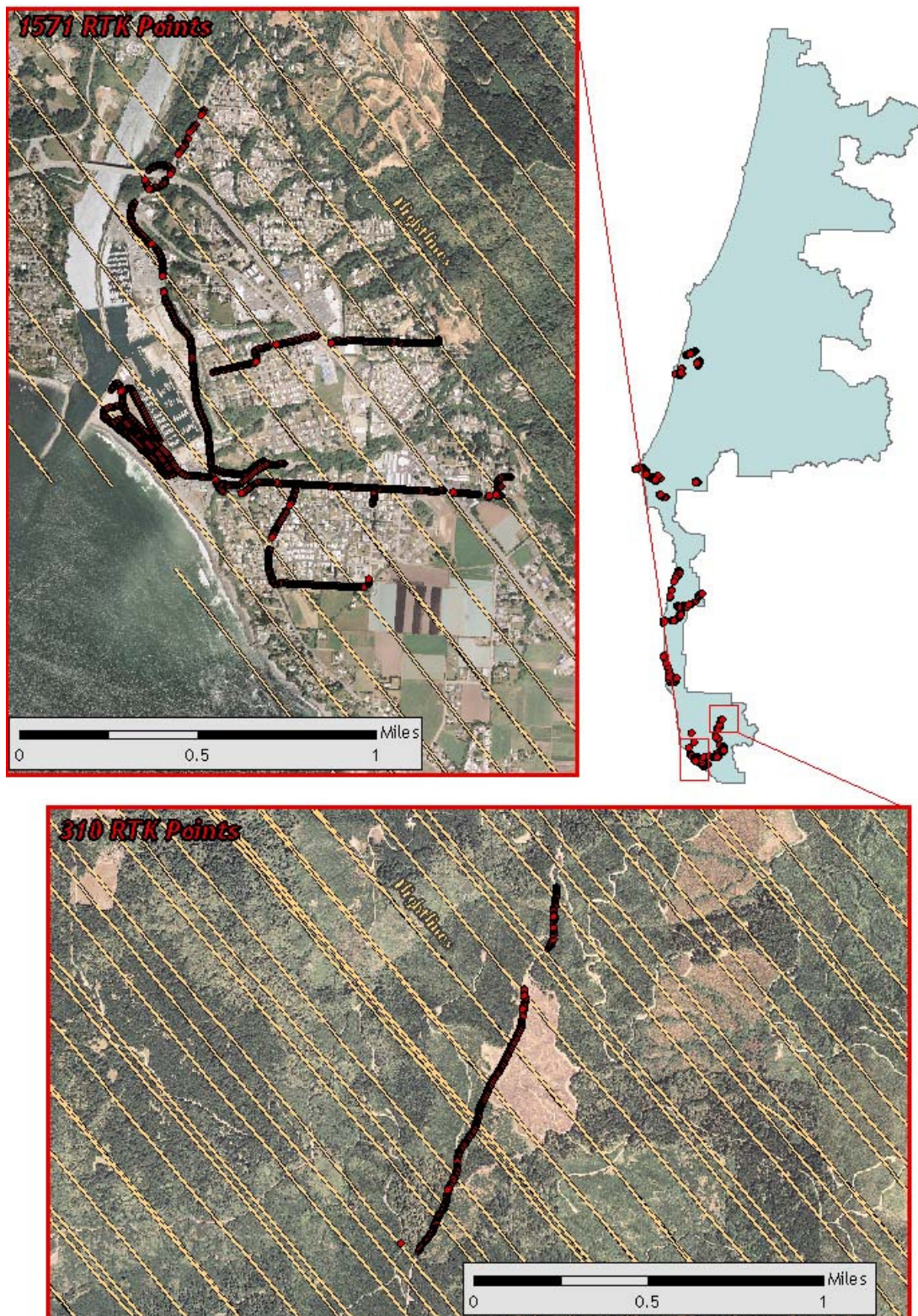


Figure 2.4. RTK point locations in the study area; images are NAIP Orthoimages.

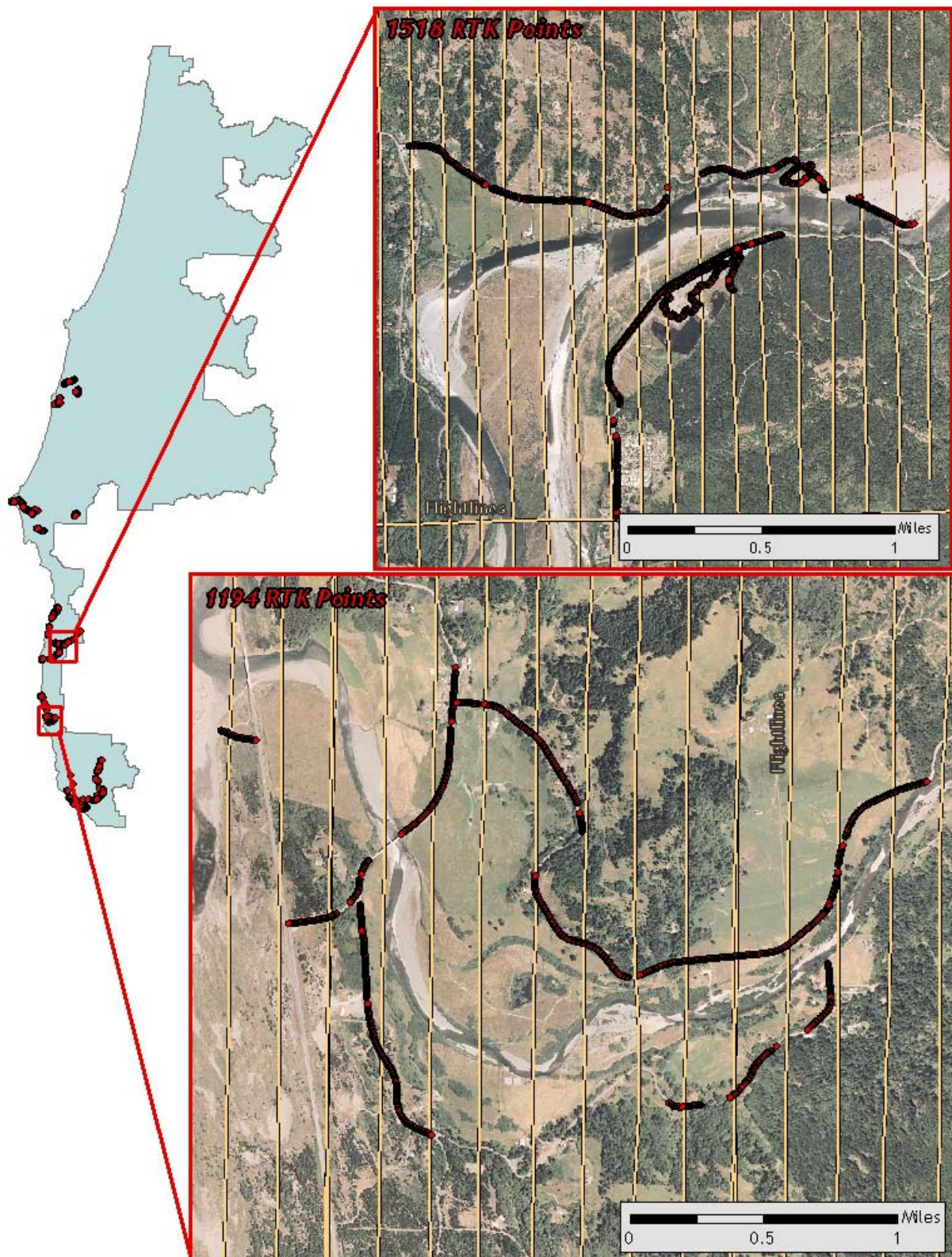
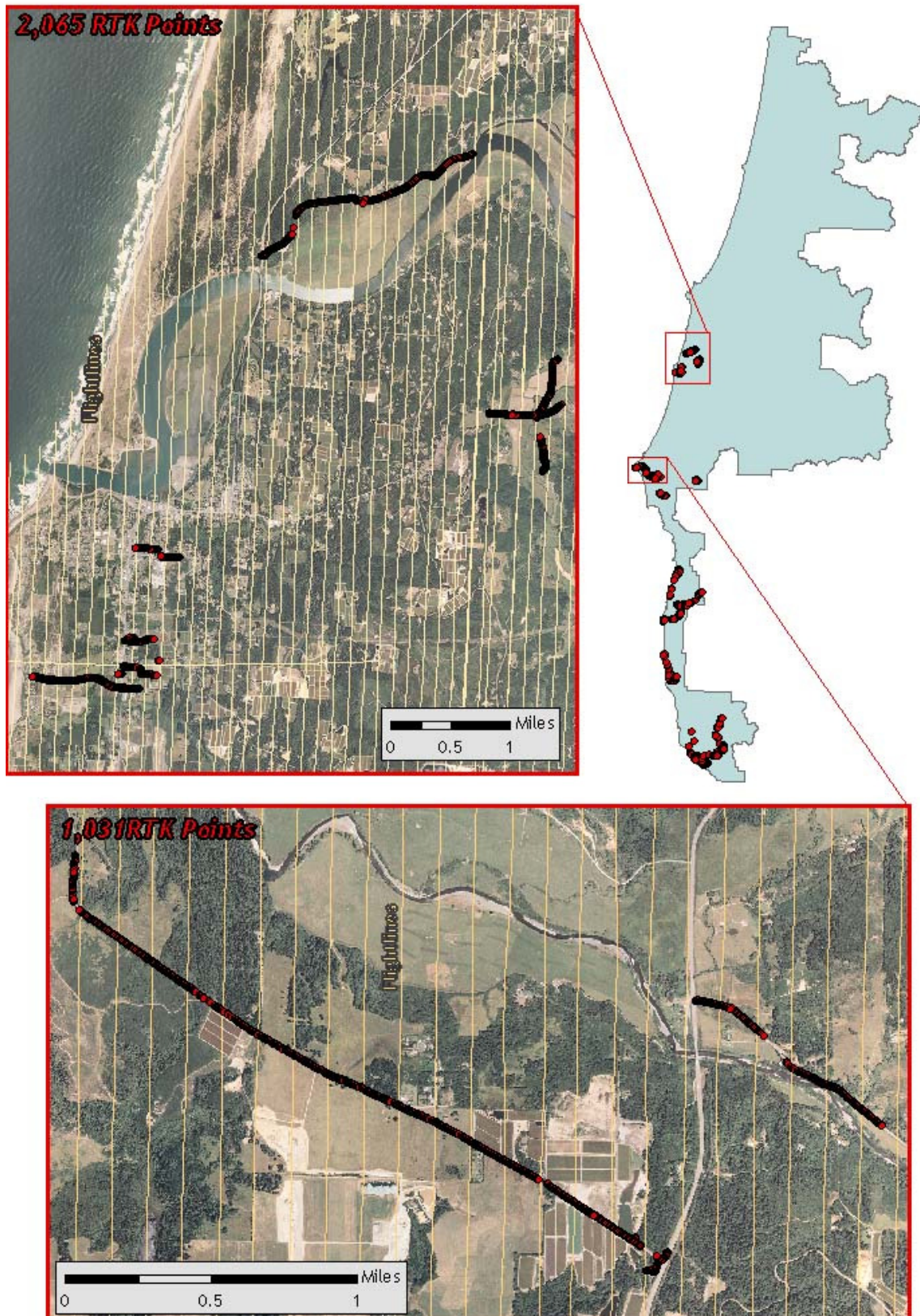


Figure 2.5. RTK point locations in the study area; images are NAIP Orthoimages.



3. LiDAR Data Processing

3.1 Applications and Work Flow Overview

1. Resolve kinematic corrections for aircraft position data using kinematic aircraft GPS and static ground GPS data.
Software: Waypoint GPS v.7.80, Trimble Geomatics Office v.1.62
2. Develop a smoothed best estimate of trajectory (SBET) file that blends the post-processed aircraft position with attitude data. Sensor head position and attitude are calculated throughout the survey. The SBET data are used extensively for laser point processing.
Software: IPAS v.1.4
3. Calculate laser point position by associating the SBET position to each laser point return time, scan angle, intensity, etc. Creates raw laser point cloud data for the entire survey in *.las (ASPRS v1.1) format.
Software: ALS Post Processing Software
4. Import raw laser points into manageable blocks (less than 500 MB) to perform manual relative accuracy calibration and filter for pits/birds. Ground points are then classified for individual flight lines (to be used for relative accuracy testing and calibration).
Software: TerraScan v.8.001
5. Using ground classified points per each flight line, the relative accuracy is tested. Automated line-to-line calibrations are then performed for system attitude parameters (pitch, roll, heading), mirror flex (scale) and GPS/IMU drift. Calibrations are performed on ground classified points from paired flight lines. Every flight line is used for relative accuracy calibration.
Software: TerraMatch v.8.001
6. Position and attitude data are imported. Resulting data are classified as ground and non-ground points. Statistical absolute accuracy is assessed via direct comparisons of ground classified points to ground RTK survey data. Data are then converted to orthometric elevations (NAVD88) by applying a Geoid03 correction. Ground models are created as a triangulated surface and exported as ArcInfo ASCII grids at a 3-foot pixel resolution.
Software: TerraScan v.8.001, ArcMap v9.2, TerraModeler v.8.001

3.2 Aircraft Kinematic GPS and IMU Data

LiDAR survey datasets are referenced to 1 Hz static ground GPS data collected over pre-surveyed monuments with known coordinates. While surveying, the aircraft collects 2 Hz kinematic GPS data. The onboard inertial measurement unit (IMU) collects 200 Hz aircraft attitude data. Waypoint GPS v.7.80 is used to process the kinematic corrections for the aircraft. The static and kinematic GPS data are then post-processed after the survey to obtain an accurate GPS solution and aircraft positions. IPAS v.1.4 is used to develop a trajectory file that includes corrected aircraft position and attitude information. The trajectory data for the entire flight survey session are incorporated into a final smoothed best estimated trajectory (SBET) file that contains accurate and continuous aircraft positions and attitudes.

3.3 Laser Point Processing

Laser point coordinates are computed using the IPAS and ALS Post Processor software suites based on independent data from the LiDAR system (pulse time, scan angle), and aircraft trajectory data (SBET). Laser point returns (first through fourth) are assigned an associated (x, y, z) coordinate along with unique intensity values (0-255). The data are output into large LAS v. 1.1 files; each point maintains the corresponding scan angle, return number (echo), intensity, and x, y, z (easting, northing, and elevation) information.

These initial laser point files are too large to process. To facilitate laser point processing, bins (polygons) are created to divide the dataset into manageable sizes (< 500 MB). Flightlines and LiDAR data are then reviewed to ensure complete coverage of the study area and positional accuracy of the laser points.

Once the laser point data are imported into bins in TerraScan, a manual calibration is performed to assess the system offsets for pitch, roll, heading and mirror scale. Using a geometric relationship developed by Watershed Sciences, each of these offsets is resolved and corrected if necessary.

The LiDAR points are then filtered for noise, pits and birds by screening for absolute elevation limits, isolated points and height above ground. Each bin is then inspected for pits and birds manually; spurious points are removed. For a bin containing approximately 7.5-9.0 million points, an average of 50-100 points are typically found to be artificially low or high. These spurious non-terrestrial laser points must be removed from the dataset. Common sources of non-terrestrial returns are clouds, birds, vapor, and haze.

The internal calibration is refined using TerraMatch. Points from overlapping lines are tested for internal consistency and final adjustments are made for system misalignments (i.e., pitch, roll, heading offsets and mirror scale). Automated sensor attitude and scale corrections yield 3-5 cm improvements in the relative accuracy. Once the system misalignments are corrected, vertical GPS drift is then resolved and removed per flight line, yielding a slight improvement (<1 cm) in relative accuracy. At this point in the workflow, data have passed a robust calibration designed to reduce inconsistencies from multiple sources (i.e., sensor attitude offsets, mirror scale, GPS drift) using a procedure that is comprehensive (i.e., uses all of the overlapping survey data).

The TerraScan software suite is designed specifically for classifying near-ground points (Soininen, 2004). The processing sequence begins by 'removing' all points that are not 'near' the earth based on geometric constraints used to evaluate multi-return points. The resulting bare earth (ground) model is visually inspected and additional ground point modeling is performed in site-specific areas (over a 50-meter radius) to improve ground detail. This is only done in areas with known ground modeling deficiencies, such as: bedrock outcrops, cliffs, deeply incised stream banks, and dense vegetation. In some cases, ground point classification includes known vegetation (i.e., understory, low/dense shrubs, etc.) and these points are manually reclassified as non-grounds. Ground surface rasters are developed from triangulated irregular networks (TINs) of ground points.

4. LiDAR Accuracy and Resolution

4.1 Laser Point Accuracy

Laser point absolute accuracy is largely a function of internal consistency (measured as relative accuracy) and laser noise:

- **Laser Noise:** For any given target, laser noise is the breadth of the data cloud per laser return (i.e., last, first, etc.). Lower intensity surfaces (roads, rooftops, still/calm water) experience higher laser noise. The laser noise range for this mission is approximately 0.02 meters.
- **Relative Accuracy:** Internal consistency refers to the ability to place a laser point in the same location over multiple flight lines, GPS conditions, and aircraft attitudes.
- **Absolute Accuracy:** RTK GPS measurements taken in the study areas compared to LiDAR point data.

Statements of statistical accuracy apply to fixed terrestrial surfaces only, not to free-flowing or standing water surfaces, moving automobiles, etc.

Table 4.1. *LiDAR accuracy is a combination of several sources of error. These sources of error are cumulative. Some error sources that are biased and act in a patterned displacement can be resolved in post processing.*

Type of Error	Source	Post Processing Solution
GPS (Static/Kinematic)	Long Base Lines	None
	Poor Satellite Constellation	None
	Poor Antenna Visibility	Reduce Visibility Mask
Relative Accuracy	Poor System Calibration	Recalibrate IMU and sensor offsets/settings
	Inaccurate System	None
Laser Noise	Poor Laser Timing	None
	Poor Laser Reception	None
	Poor Laser Power	None
	Irregular Laser Shape	None

4.1.1 Relative Accuracy

Relative accuracy refers to the internal consistency of the data set and is measured as the divergence between points from different flight lines within an overlapping area. Divergence is most apparent when flight lines are opposing. When the LiDAR system is well calibrated the line to line divergence is low (<10 cm). Internal consistency is affected by system attitude offsets (pitch, roll and heading), mirror flex (scale), and GPS/IMU drift.

Operational measures taken to improve relative accuracy:

1. Low Flight Altitude: Terrain following was targeted at a flight altitude of 900 meters above ground level (AGL). Laser horizontal errors are a function of flight altitude above ground. Lower flight altitudes decrease laser noise on surfaces with even the slightest relief.
2. Focus Laser Power at narrow beam footprint: A laser return must be received by the system above a power threshold to accurately record a measurement. The strength of the laser return is a function of laser emission power, laser footprint, flight altitude and the reflectivity of the target. While surface reflectivity cannot be controlled, laser power can be increased and low flight altitudes can be maintained.
3. Reduced Scan Angle: Edge-of-scan data can become inaccurate. The scan angle was reduced to a maximum of $\pm 14^\circ$ from nadir, creating a narrow swath width and greatly reducing laser shadows from trees and buildings.
4. Quality GPS: Flights took place during optimal GPS conditions (e.g., 6 or more satellites and PDOP [Position Dilution of Precision] less than 3.0). Before each flight, the PDOP was determined for the survey day. During all flight times, a dual frequency DGPS base station recording at 1-second epochs was utilized and a maximum baseline length between the aircraft and the control points was less than 19 km (11.5 miles) at all times.
5. Ground Survey: Ground survey point accuracy increases during optimal PDOP ranges and targets a minimal baseline distance of 4 miles between GPS rover and base. Robust statistics are, in part, a function of sample size (n) and distribution. The ground survey collected 12,377 RTK points that are distributed throughout multiple flight lines across the study areas.
6. 50% Side-Lap (100% Overlap): Overlapping areas are optimized for relative accuracy testing. Laser shadowing is minimized to help increase target acquisition from multiple scan angles. Ideally, with a 50% side-lap, the most nadir portion of one flight line coincides with the edge (least nadir) portion of overlapping flight lines. A minimum of 50% side-lap with terrain-followed acquisition prevents data gaps.
7. Opposing Flight Lines: All overlapping flight lines are opposing. Pitch, roll and heading errors are amplified by a factor of two relative to the adjacent flight line(s), making misalignments easier to detect and resolve.

Relative Accuracy Calibration Methodology

1. Manual System Calibration: Calibration procedures for each mission require solving geometric relationships that relate measured swath-to-swath deviations to misalignments of system attitude parameters. Corrected scale, pitch, roll and heading offsets are calculated and applied to resolve misalignments. The raw divergence between lines is computed after the manual calibration is completed and reported for each study area.
2. Automated Attitude Calibration: All data are tested and calibrated using TerraMatch automated sampling routines. Ground points are classified for each individual flight line and used for line-to-line testing. ***The resulting overlapping ground points (per line) total over 800 million points for Delivery 5 from which to compute and refine relative accuracy.*** System misalignment offsets (pitch, roll and heading) and mirror scale are solved for each individual mission. The application of attitude misalignment offsets (and mirror scale) occurs for each individual mission. The data from each mission are then blended when imported together to form the entire area of interest.
3. Automated Z Calibration: Ground points per line are utilized to calculate the vertical divergence between lines caused by vertical GPS drift. Automated Z calibration is the final step employed for relative accuracy calibration.

Relative Accuracy Calibration Results

The relative accuracy listed below is calculated for Delivery 5 only and is based on the comparison of 137 flightlines and over 800 million points. Future reports will include cumulative statistics for all data delivered to date.

- Delivery 5 Average = 0.23 ft
- Median Relative Accuracy = 0.24 ft
- 1σ Relative Accuracy = 0.26 ft
- 2σ Relative Accuracy = 0.45 ft

Figure 4.1. Distribution of relative accuracies per flight line, non slope-adjusted for Delivery 5.

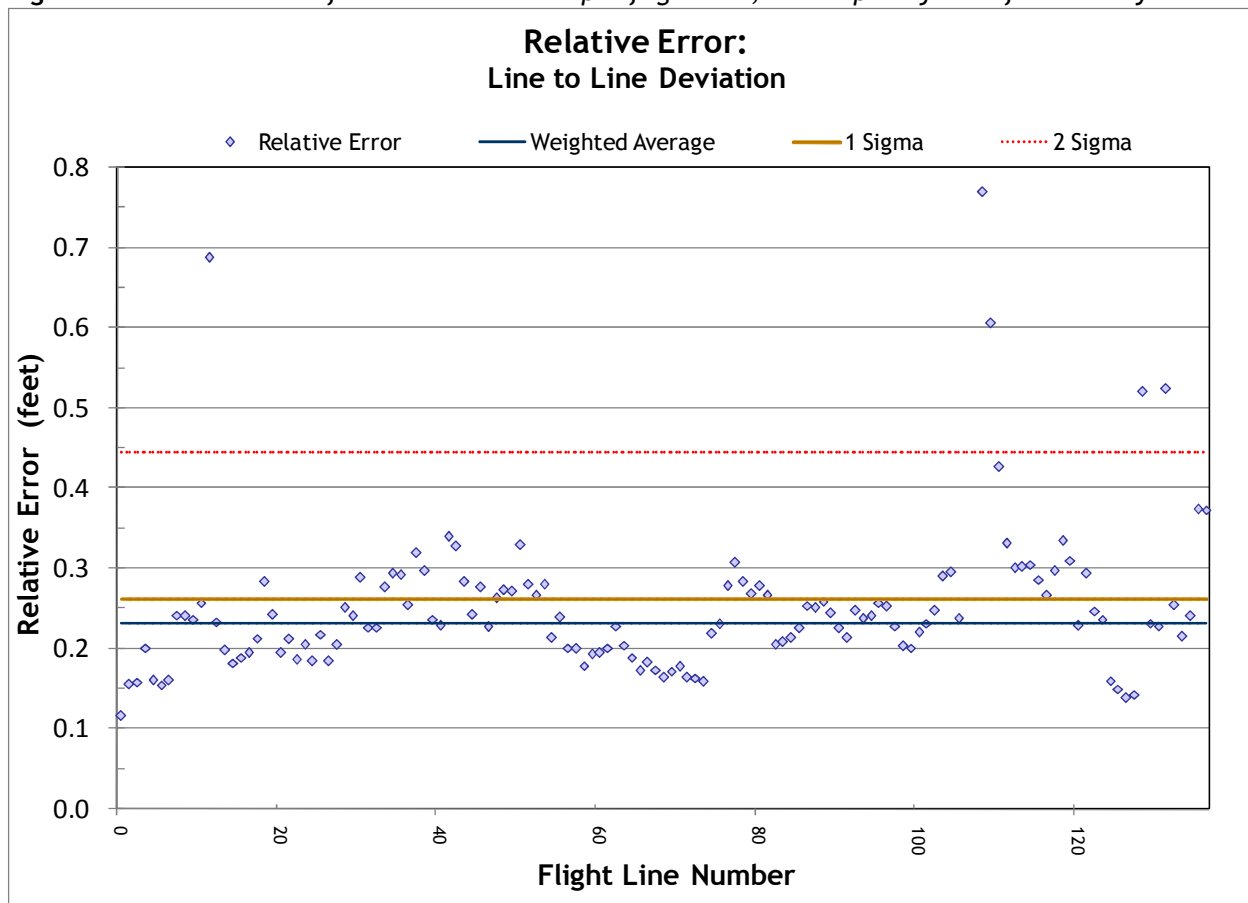


Figure 4.2. Statistical relative accuracies, non slope-adjusted for Delivery 5.

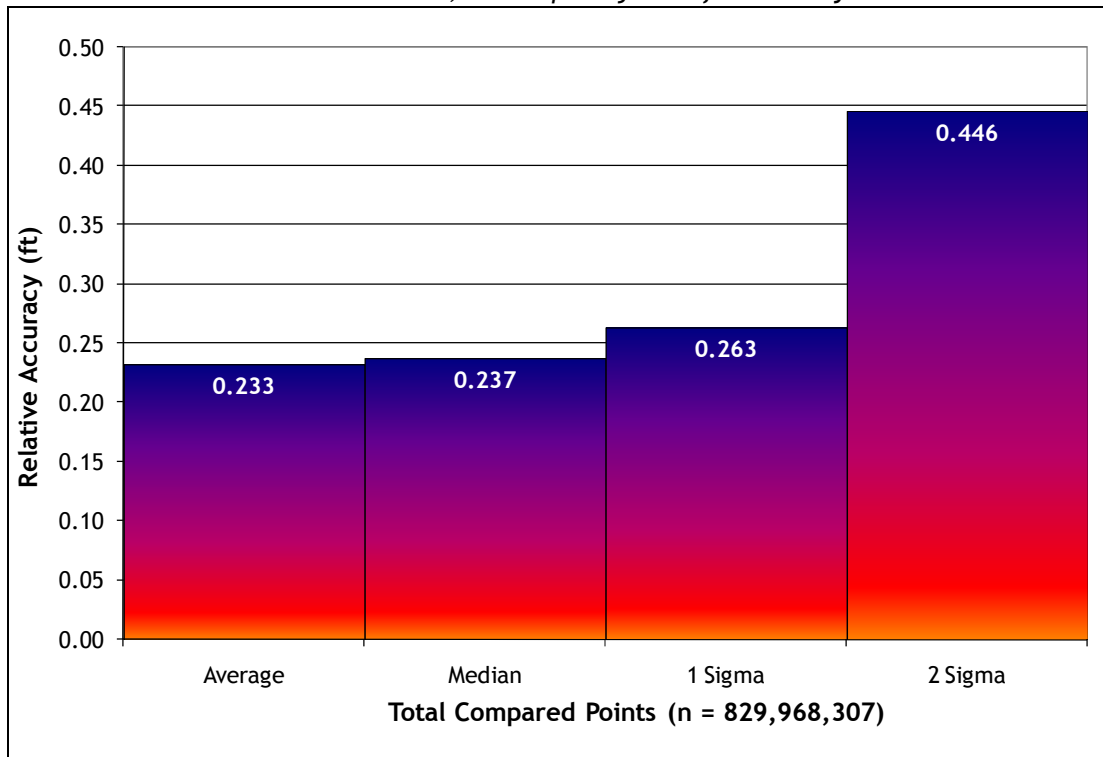
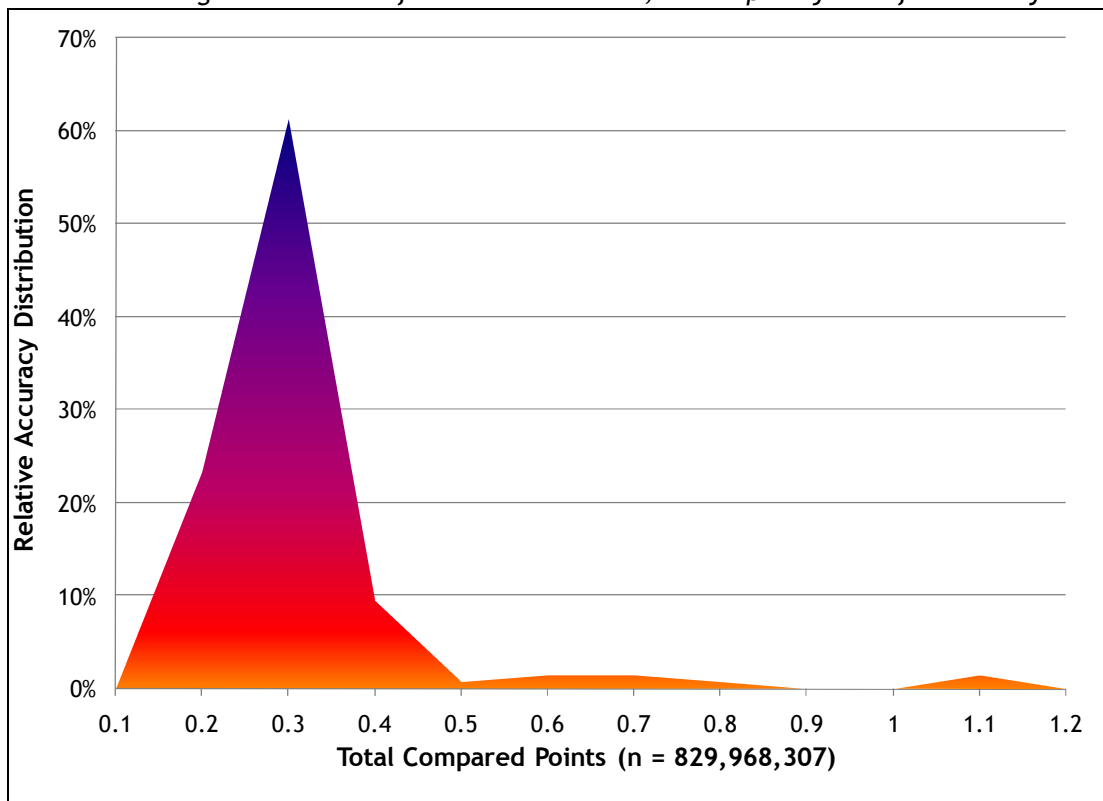


Figure 4.3. Percentage distribution of relative accuracies, non slope-adjusted for Delivery 5.



4.1.2 Absolute Accuracy

The final quality control measure is a statistical accuracy assessment that compares known RTK ground survey points to the closest laser point. For the DOGAMI southern Oregon coast study area, 12,377 RTK points were collected for data delivered to date. Accuracy statistics are reported in **Table 4.2** and shown in Figures 4.4-4.5. Accuracy statistics have been developed for the areas delivered to date.

Table 4.2. Absolute Accuracy - Deviation between laser points and RTK survey points.

Sample Size (n): 12,377	
Root Mean Square Error (RMSE): 0.15 feet	
Standard Deviations	Deviations
1 sigma (σ): 0.15 feet	Minimum Δz : -0.66 feet
2 sigma (σ): 0.34 feet	Maximum Δz : 0.57 feet
	Average Δz : -0.05 feet

Figure 4.4. Study Area: Histogram Statistics

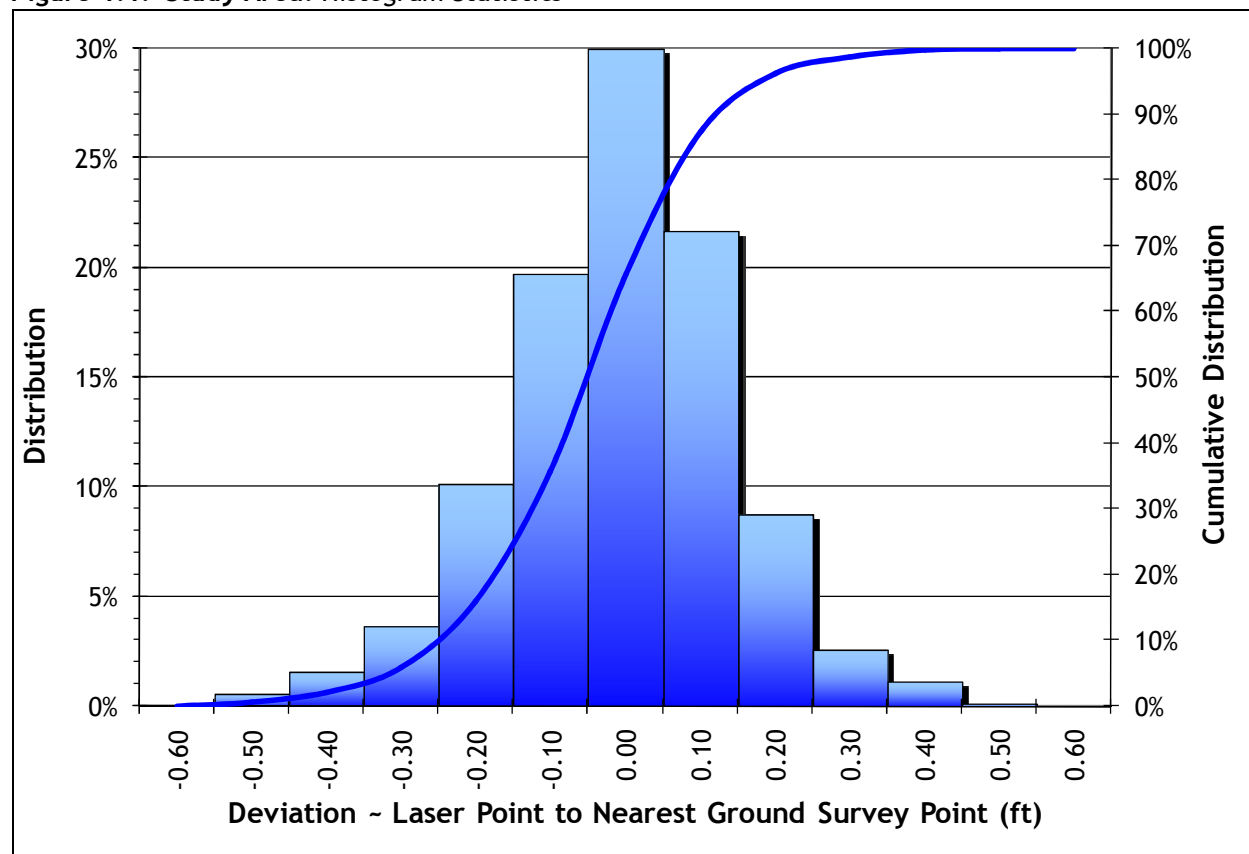
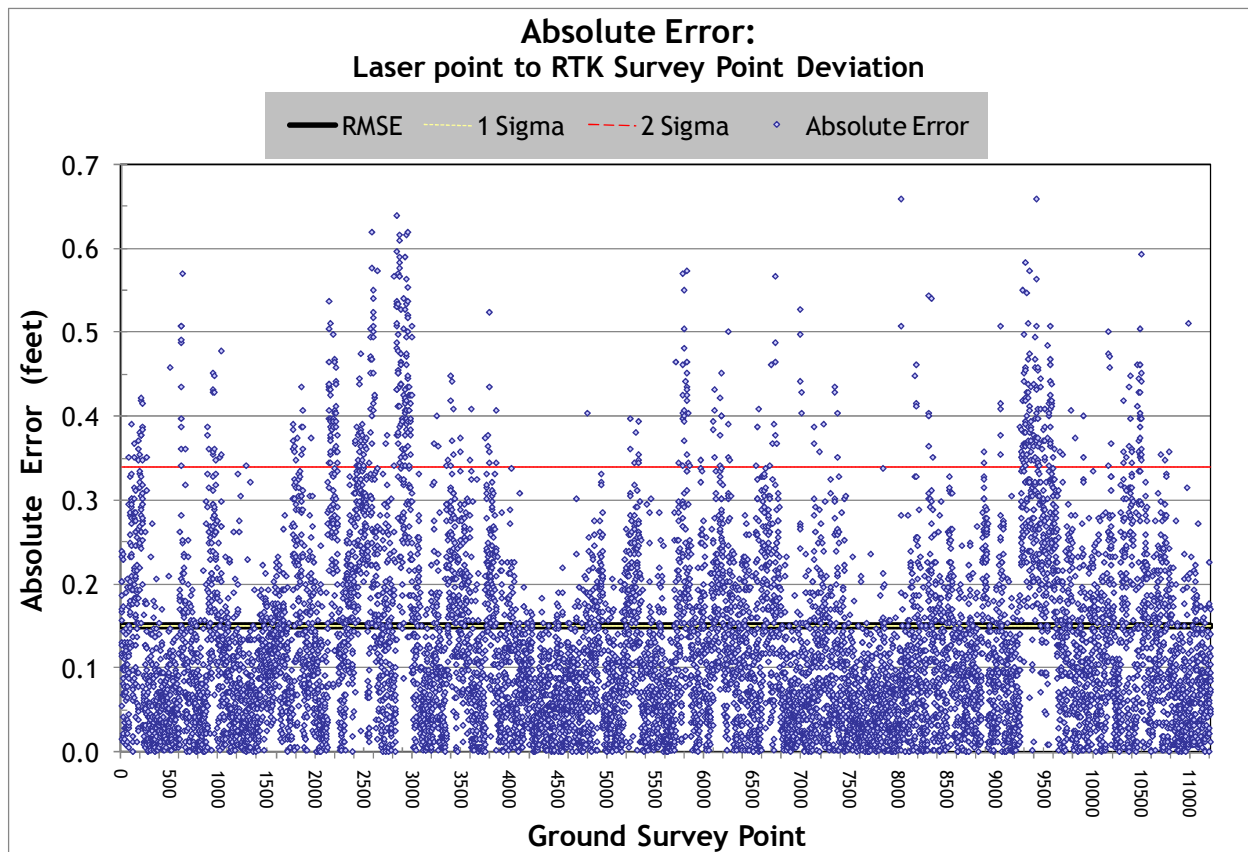


Figure 4.5. Study Area: Point Absolute Deviation Statistics



4.2 Data Density/Resolution

Some types of surfaces (i.e., dense vegetation or water) may return fewer pulses than the laser originally emitted. Therefore, the delivered density can be less than the native density and lightly variable according to distributions of terrain, land cover and water bodies. Density histograms and maps (Figures 4.6-4.9) have been calculated based on first return laser point density and ground-classified laser point density (see Section 4.3 for discussion of density per AOI).

Table 4.3. Average Densities for data delivered to date.

Average Pulse Density (per square ft)	Average Pulse Density (per square m)	Average Ground Density (per square ft)	Average Ground Density (per square m)
0.79	8.50	0.07	0.75

4.2.1 First Return Laser Pulses per Square Foot

Figure 4.6. Histogram of first return laser point density for data delivered to date.

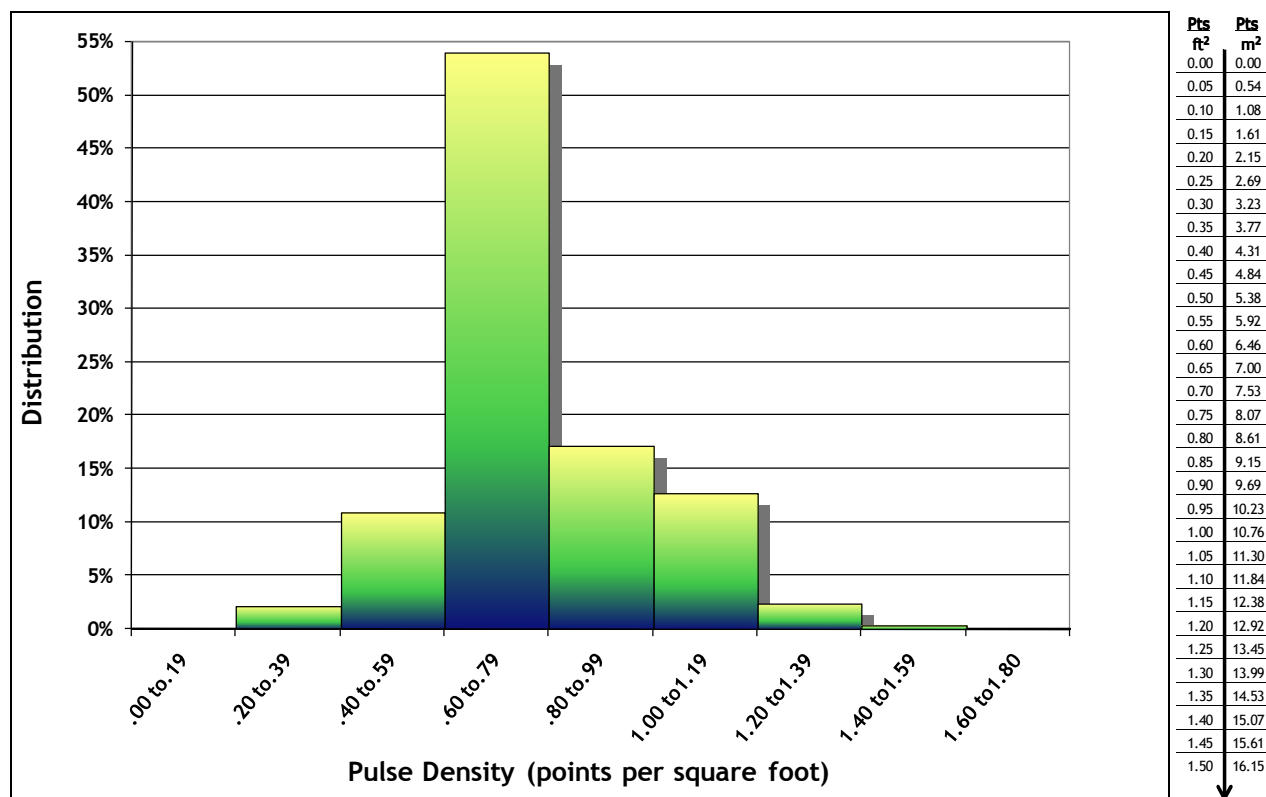
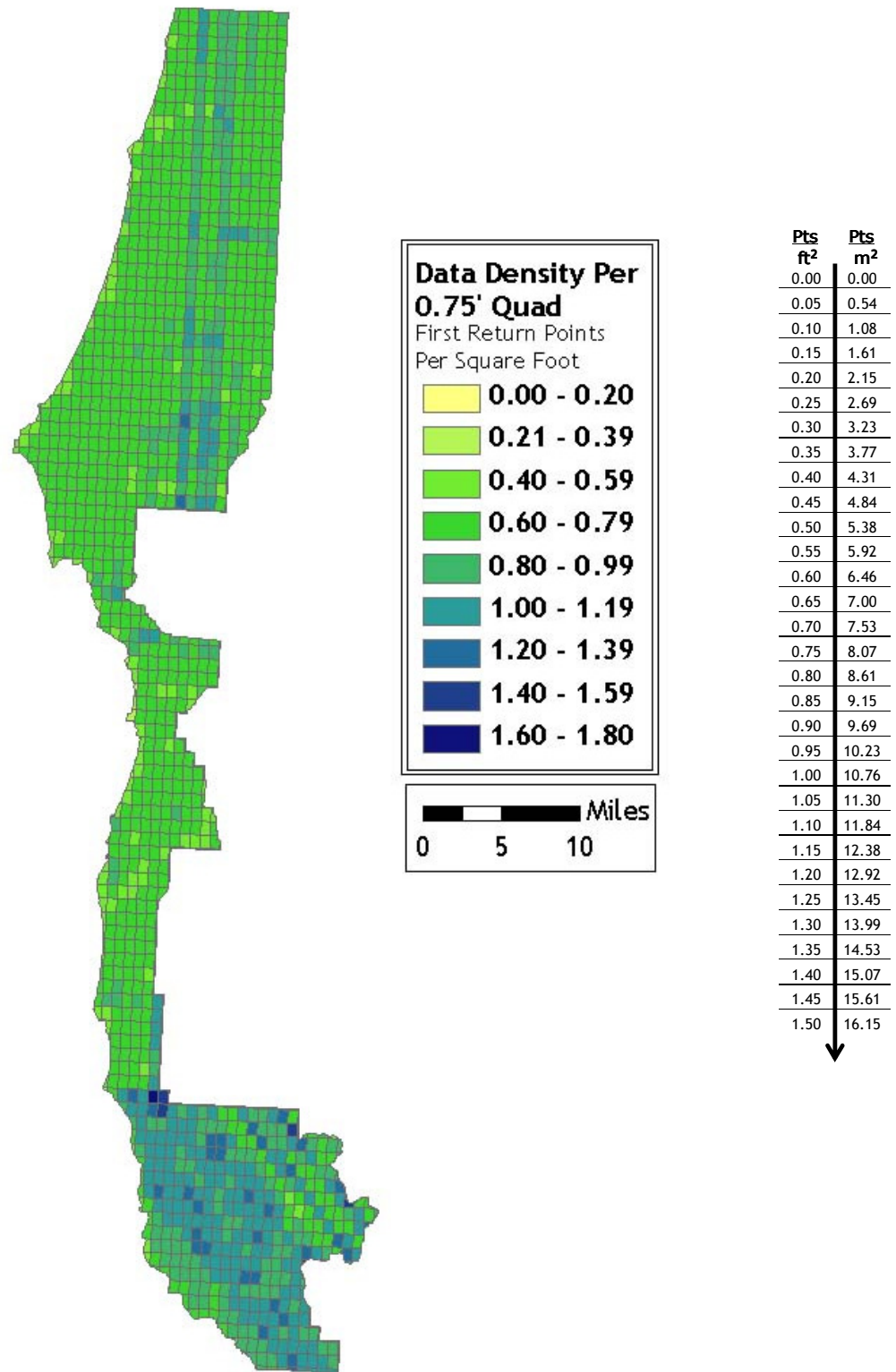


Figure 4.7. First return laser point density for data delivered to date, per 0.75' USGS Quad.



4.2.2 Classified Ground Points per Square Foot

Ground classifications are derived from ground surface modeling. Supervised classifications were performed by reseeded of the ground model where it is determined that the ground model has failed, usually under dense vegetation and/or at breaks in terrain, steep slopes and at bin boundaries.

Figure 4.8. Histogram of ground-classified laser point density for data delivered to date.

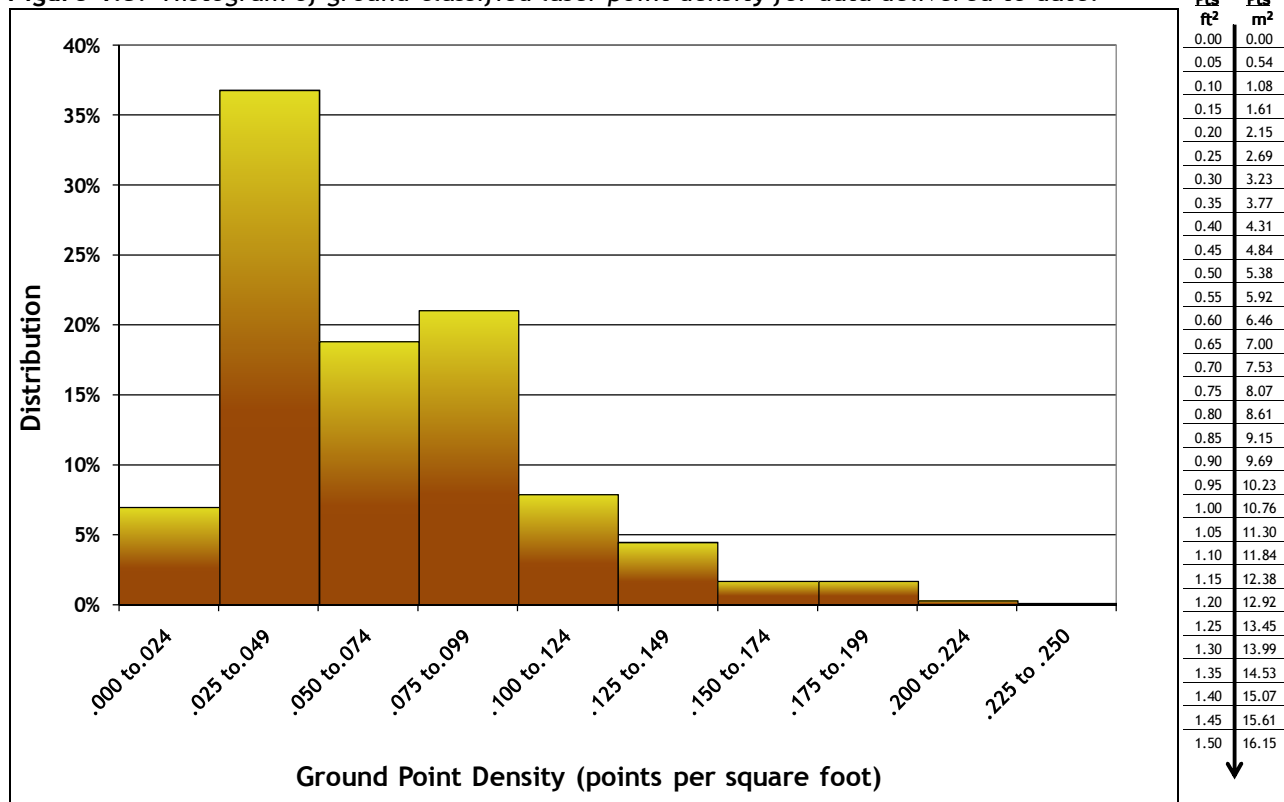
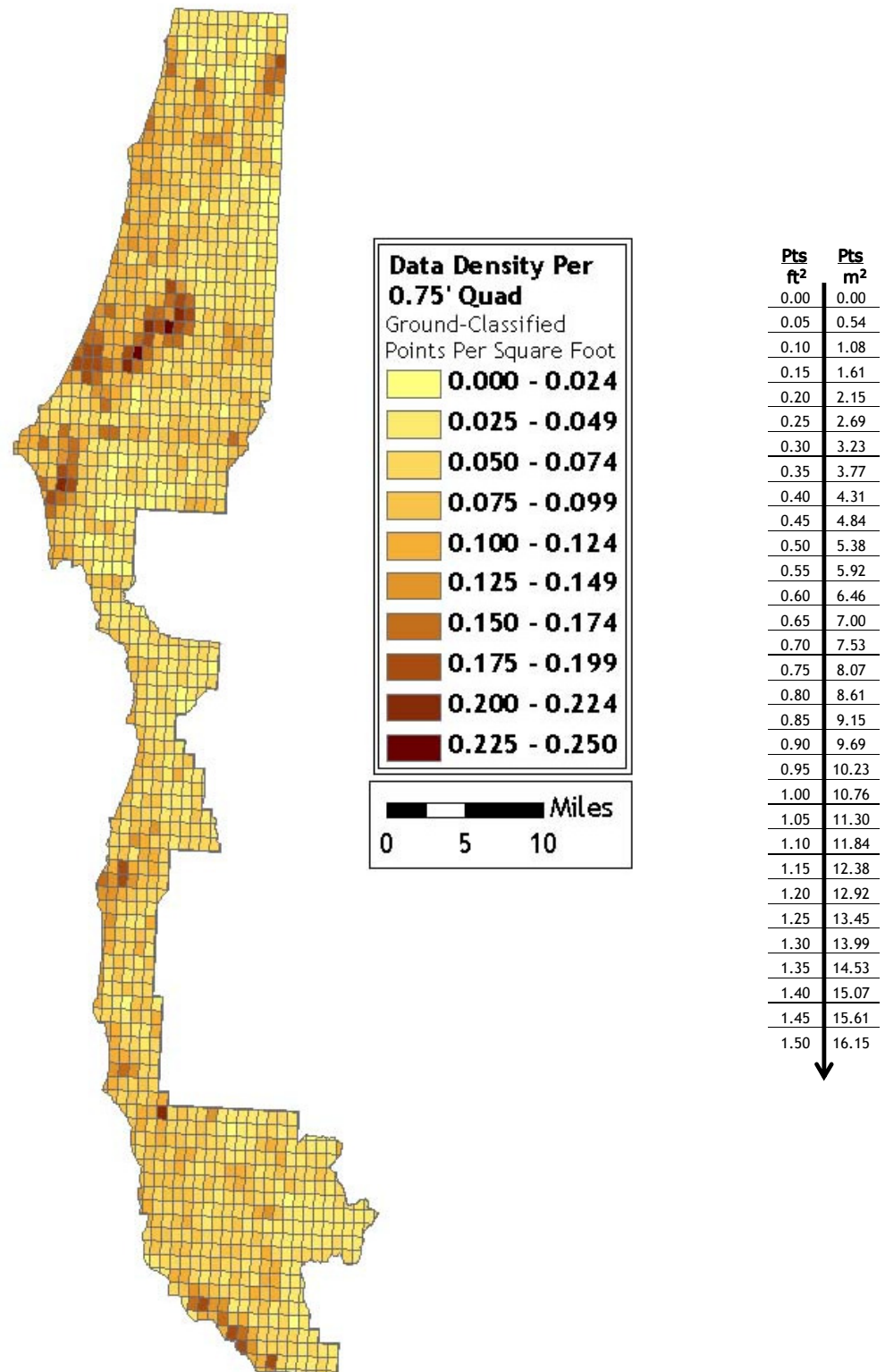


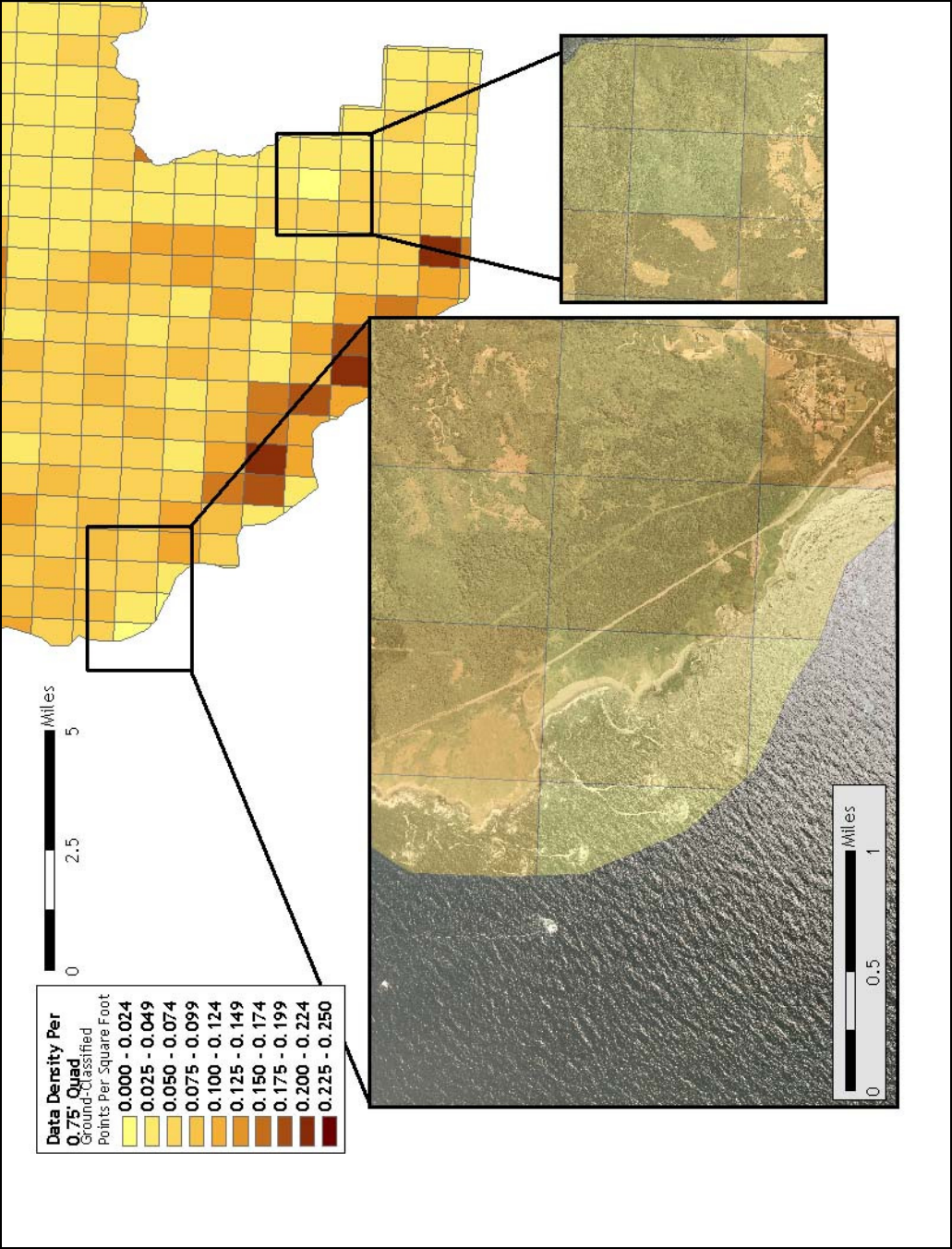
Figure 4.9. Ground-classified laser point density for data delivered to date, per 0.75' USGS Quad.



4.3 Data Density/Resolution per Delivery

4.3.1 Delivery 1

Figure 4.10. Quadrants containing few ground classified points include coastal areas and areas of dense vegetation.



4.3.2 Delivery 2

Figure 4.11. This quadrant illustrates a high number of ground classified points due to flightline overlap and areas of little or no ground cover.

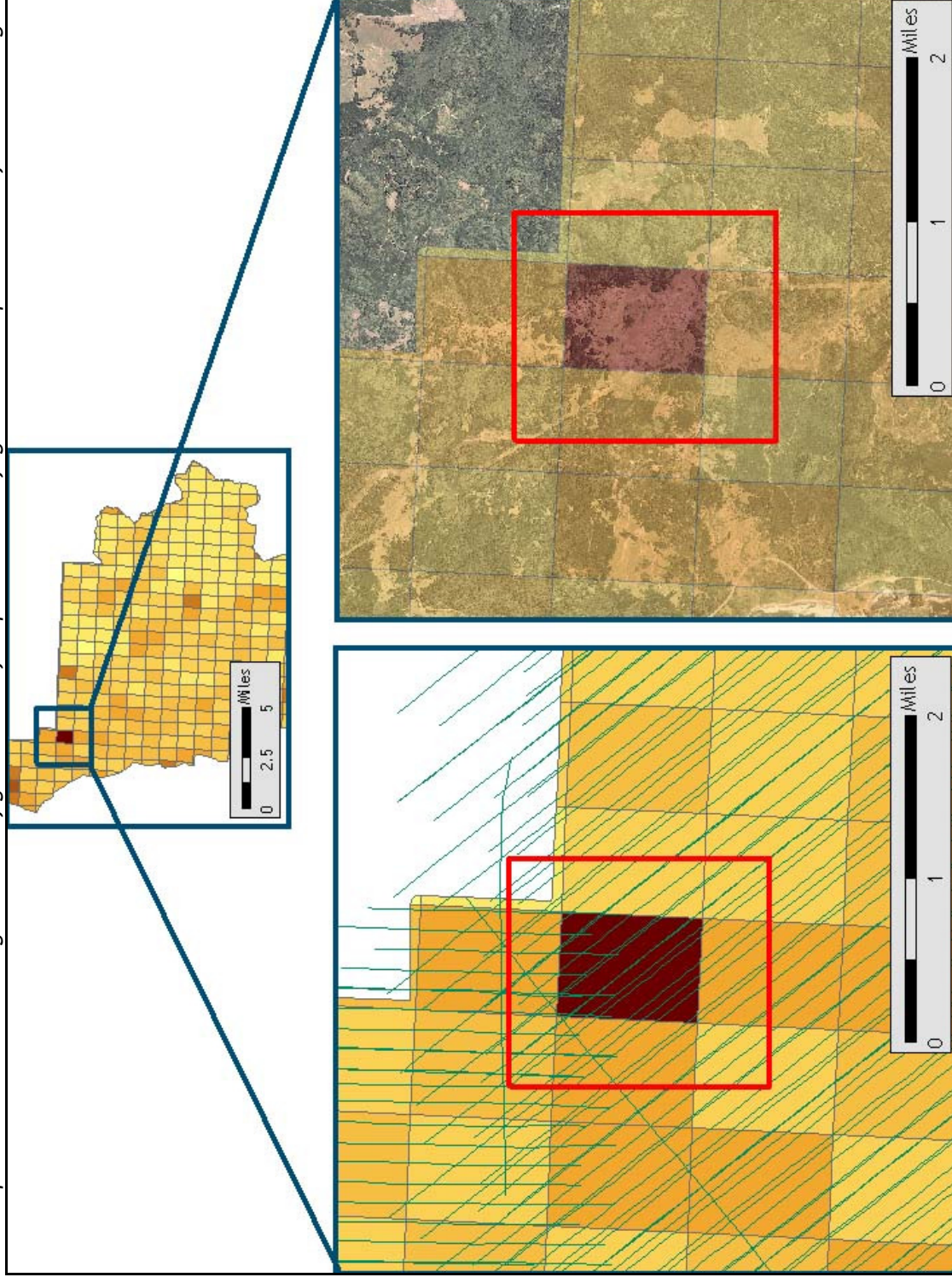
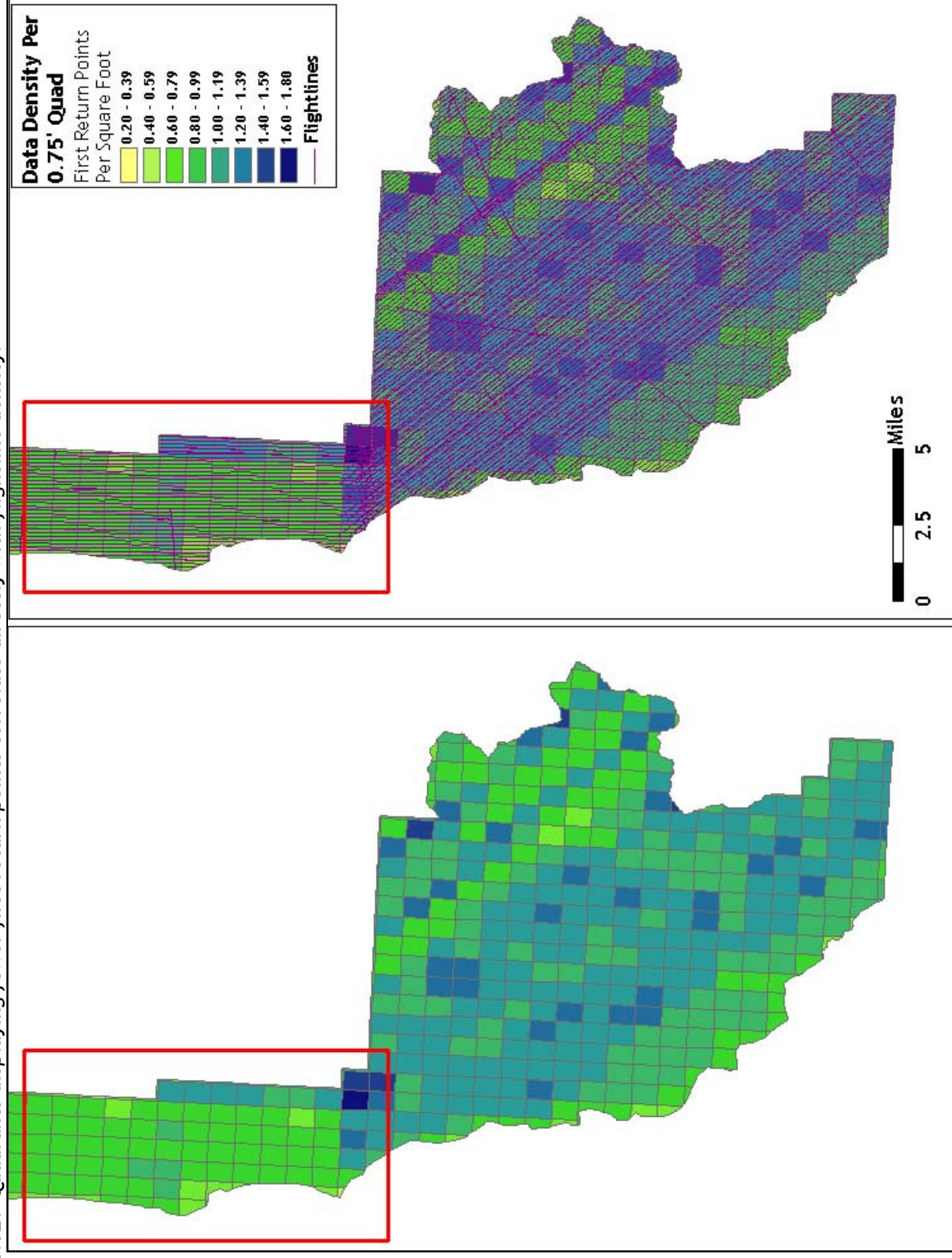
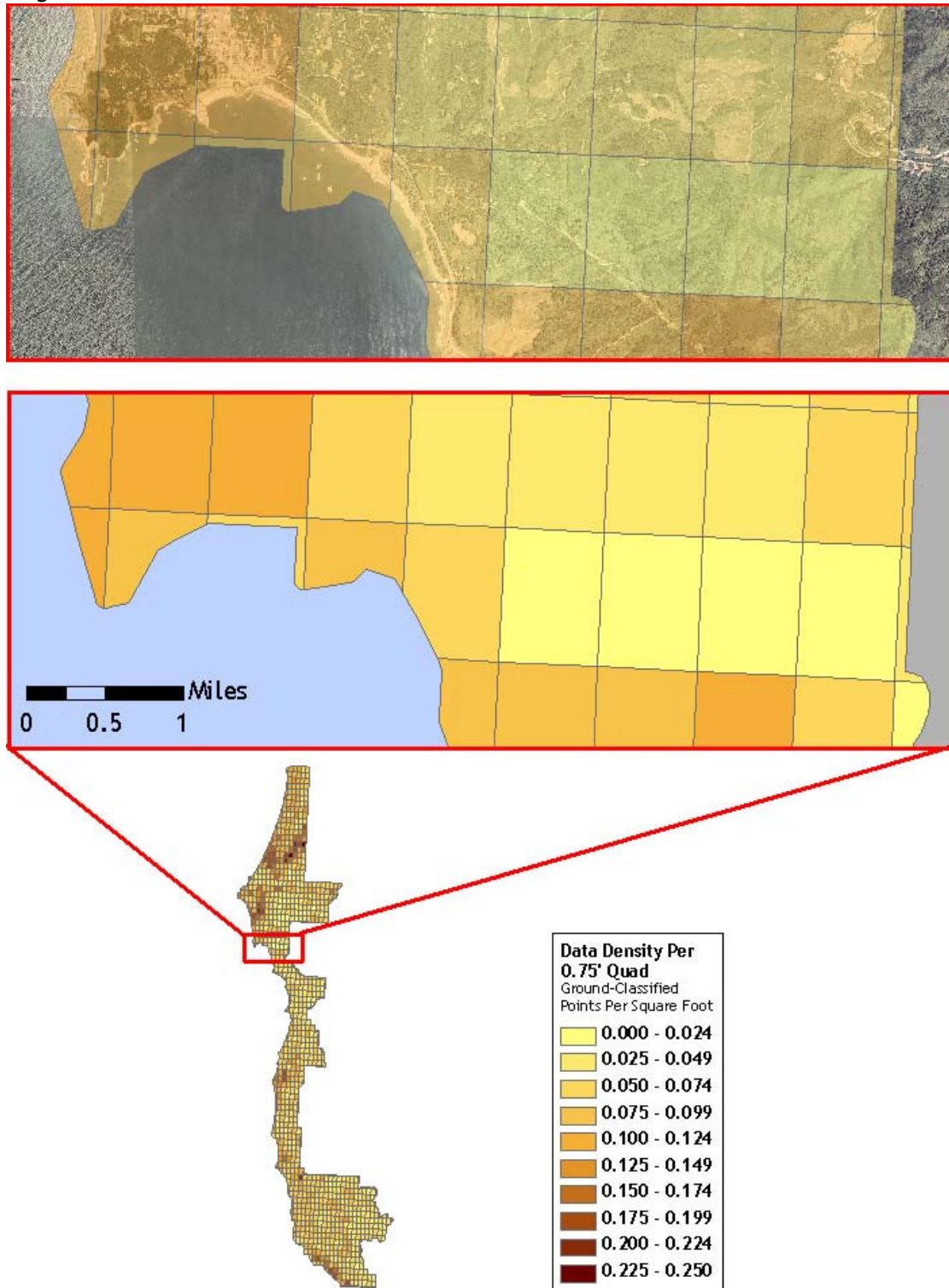


Figure 4.12. Quadrants displaying fewer first return points correlate directly with flightline density.



4.3.3 Delivery 3

Figure 4.13. Quadrants containing few ground classified points include coastal areas and areas of dense vegetation.



4.3.4 Delivery 4

Figure 4.14. Quadrants with exposed ground or little vegetation result in higher ground-classified point density.

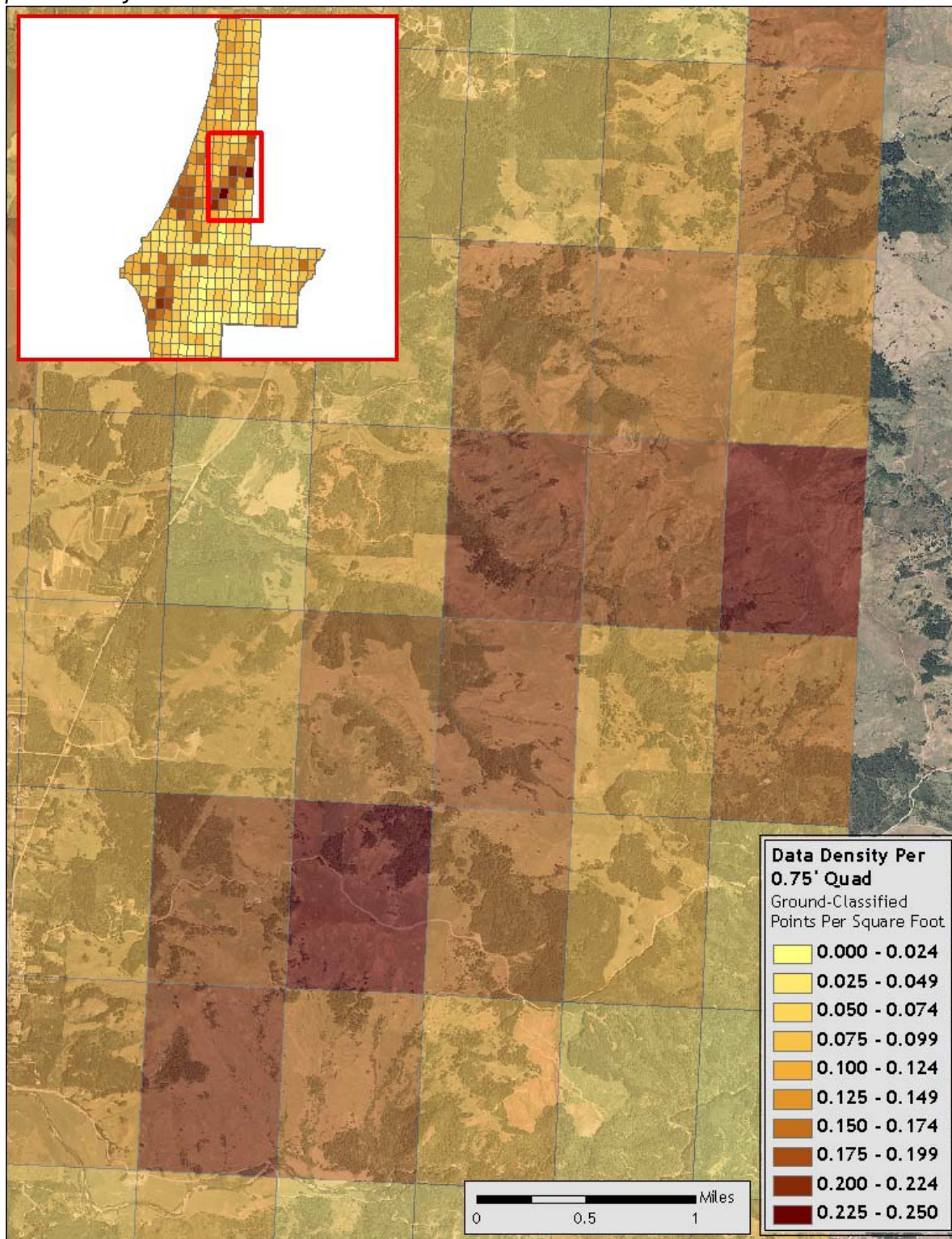
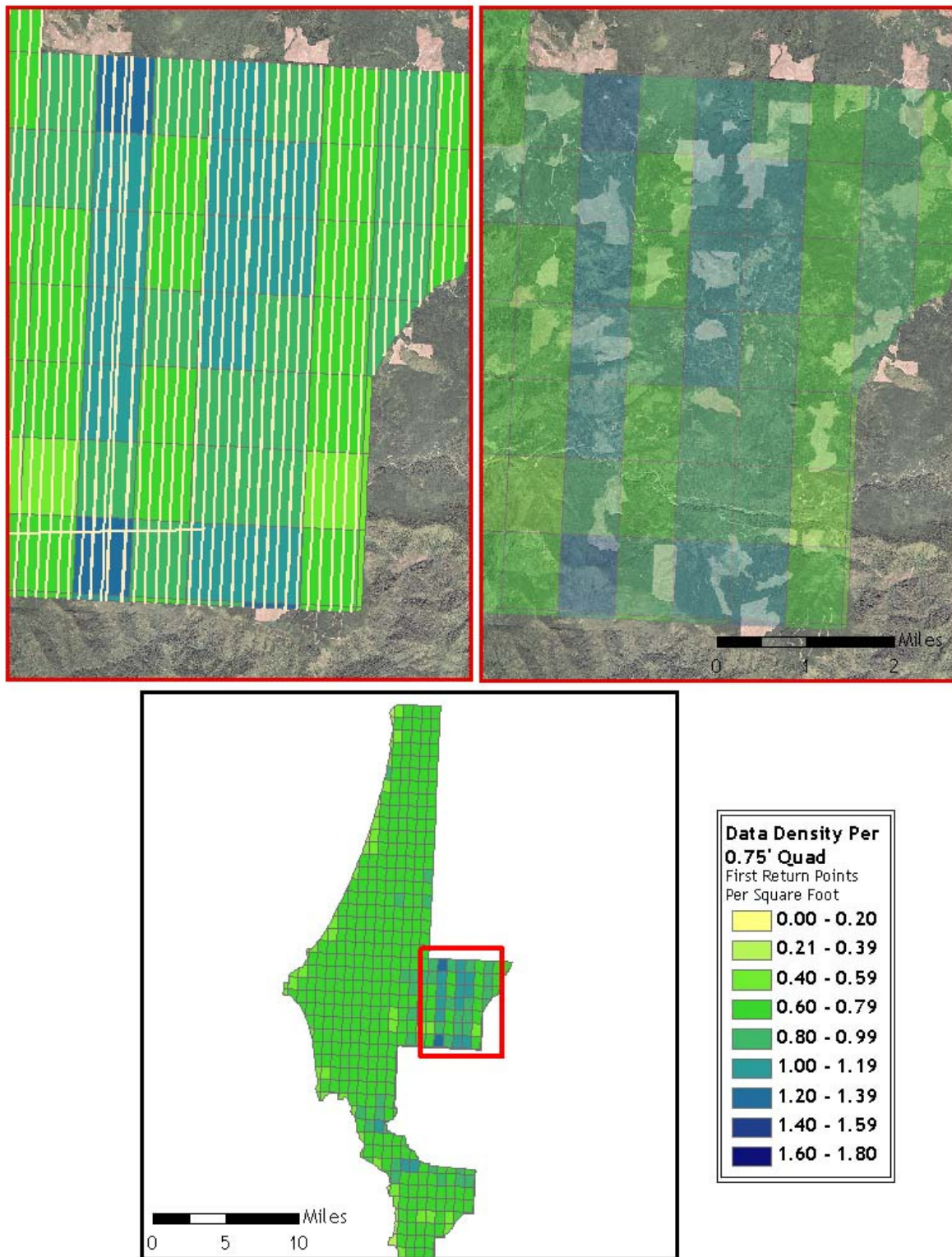


Figure 4.15. Quadrants with higher flightline density result in greater numbers of first return points.



5. Deliverables

All Deliveries of DOGAMI and ODF Data conform to the following tiling scheme:

Figure 5.1. 0.75’ USGS Quad Delineation Naming Convention.



5.1 Point Data (per 0.75' USGS Quad)

Data Fields: Number, X, Y, Z, Intensity, ReturnNumber, Class, GPSTime

- LAS v 1.1 Format

5.2 Vector Data

- Total Area Flown
 - 7.5-minute quadrangle delineation in shapefile format
 - 0.75-minute quadrangle delineation in shapefile format (See **Figure 5.1** for illustration)
- Area Delivered to date
 - Ground control point data
 - Study area shapefile

5.3 Raster Data

- ESRI GRID of Bare Earth Modeled LiDAR data Points (3-foot resolution) delivered in 7.5' USGS Quad Delineation
- ESRI GRID of Above Ground Modeled LiDAR data Points (3-foot resolution) delivered in 7.5' USGS Quad Delineation
- Intensity Images in GeoTIFF format (1.5-foot resolution) delivered per 0.75' Quad
- Ground Density Rasters in GeoTIFF format (3-foot resolution) delivered per 0.75' Quad

5.4 Data Report

- Full Report containing introduction, methodology, and accuracy.
 - Word Format (*.doc)
 - PDF Format (*.pdf)

5.5 Datum and Projection

The data were processed as ellipsoidal elevations and required a Geoid transformation to be converted into orthometric elevations (NAVD88). In TerraScan, the NGS published Geoid03 model is applied to each point. The data were processed using meters in the Universal Transverse Mercator (UTM) Zone 10 and NAD83 (CORS96)/NAVD88 datum and converted to the following projections.

- DOGAMI data are delivered in Oregon Lambert (NAD 83), with horizontal and vertical units in International Feet, in the NAD83 HARN/NAVD88 datum (Geoid 03).

6. Selected Imagery

Example areas are presented to show sample imagery (see **Figures 6.1-6.9**).

Figure 6.1. View to Northwest at oceanside near Harris Beach State Park, Oregon (quad 42124-A3). Top image derived from highest hit LiDAR, lower image derived from bare earth LiDAR.

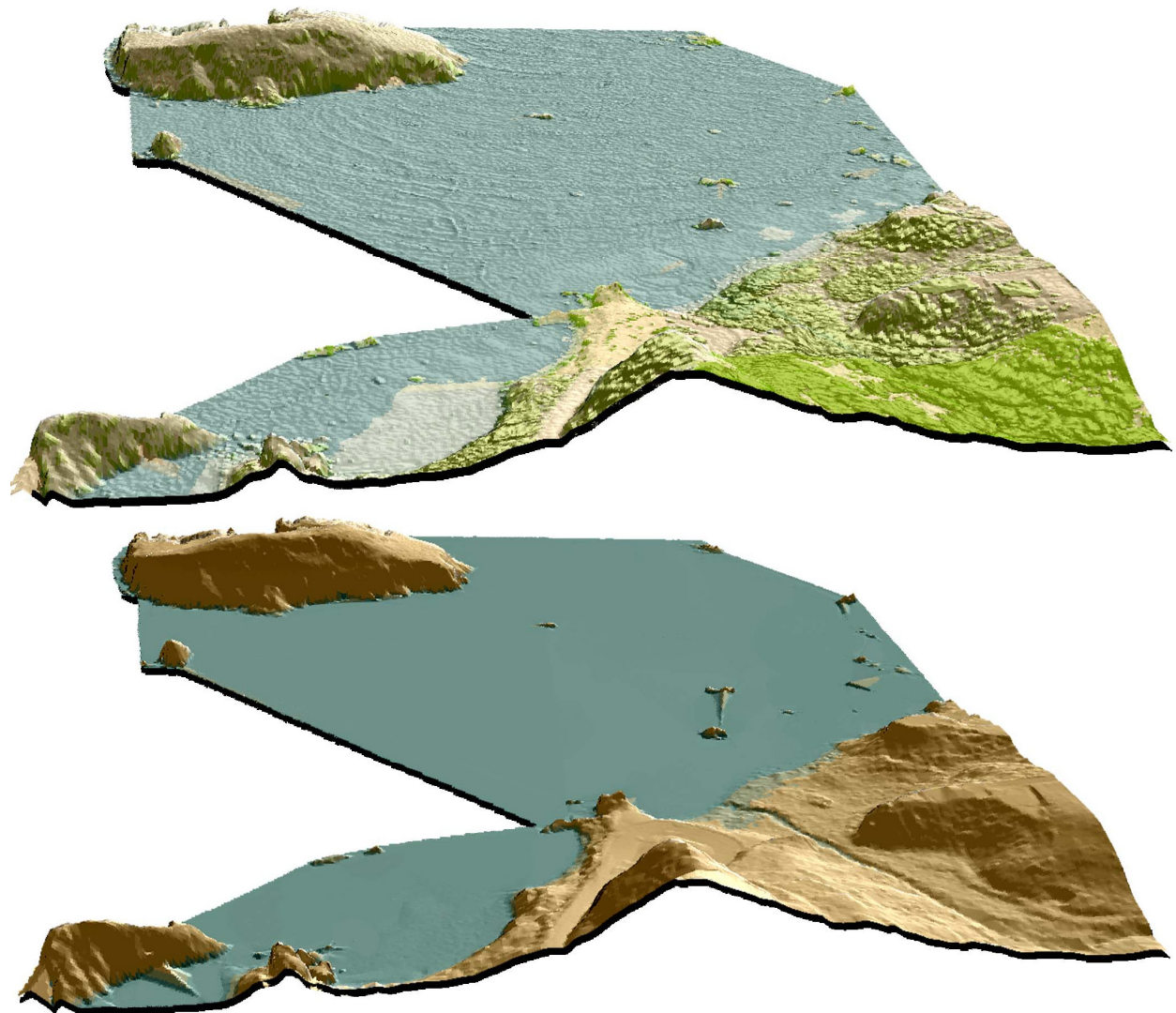


Figure 6.2. View to Southeast and upstream along Chetco River at its confluence with Jack Creek (quad 42124-A2). Top image is derived from highest hit LiDAR, lower image derived from bare earth LiDAR.

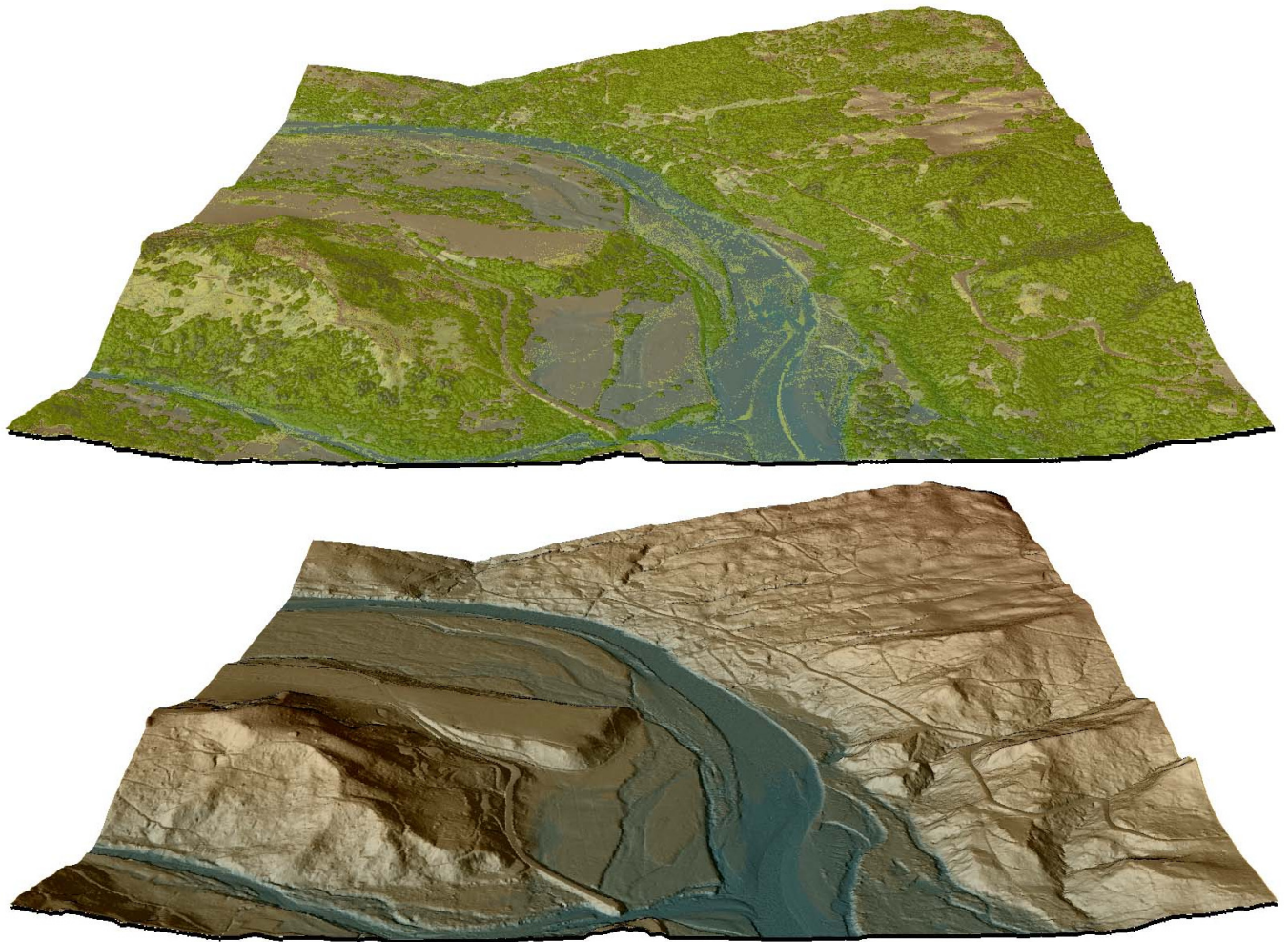


Figure 6.3. View upstream and to Northeast of Chetco River at confluence with North Fork Chetco River (quad 42124-a2). Top image derived from highest hit LiDAR, lower image derived from bare earth LiDAR.

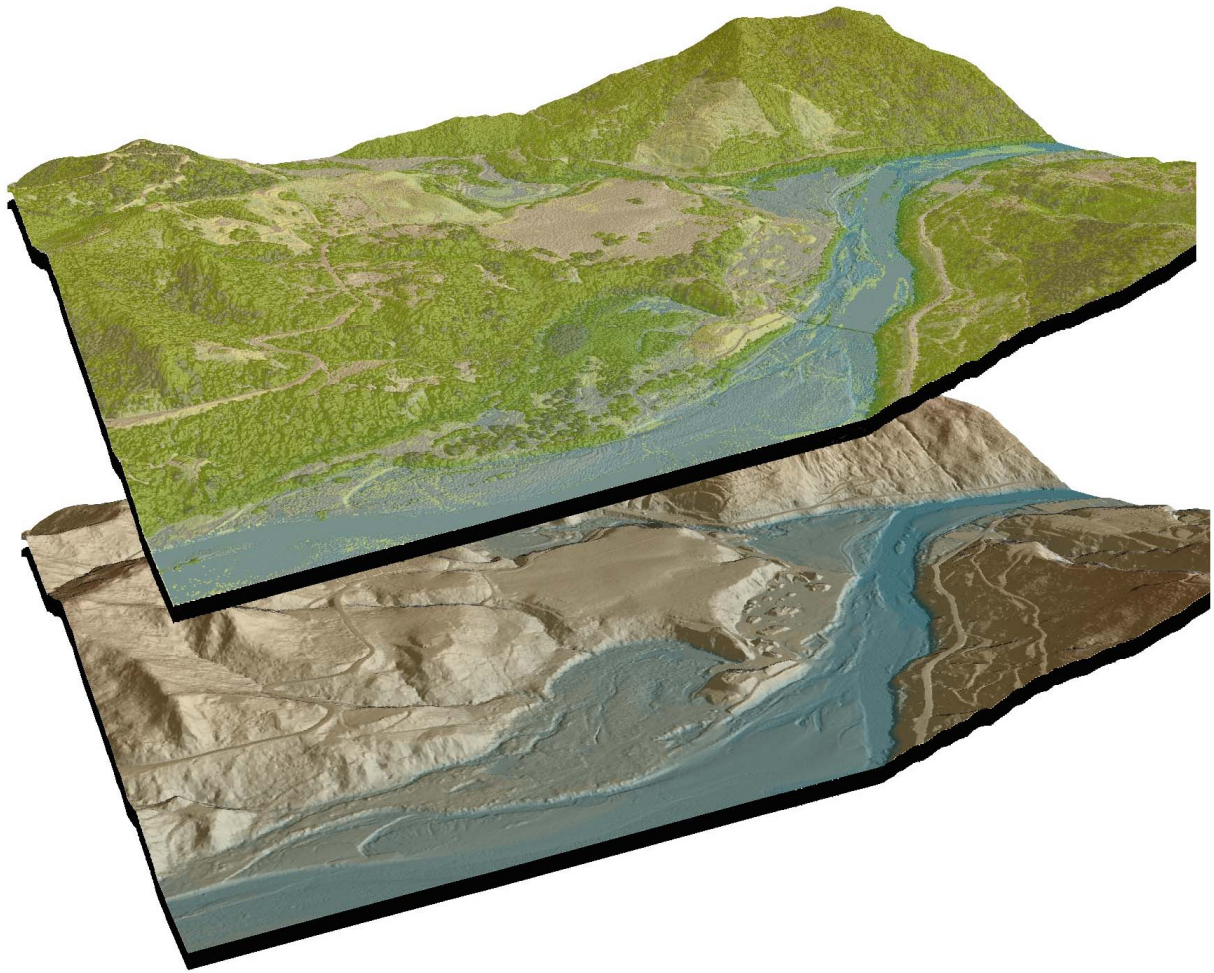


Figure 6.4. Oblique view of coastline at confluence of Whalehead Creek and ocean (quad 42124-b3). Upper image derived from highest hit LiDAR, lower image derived from bare earth LiDAR.

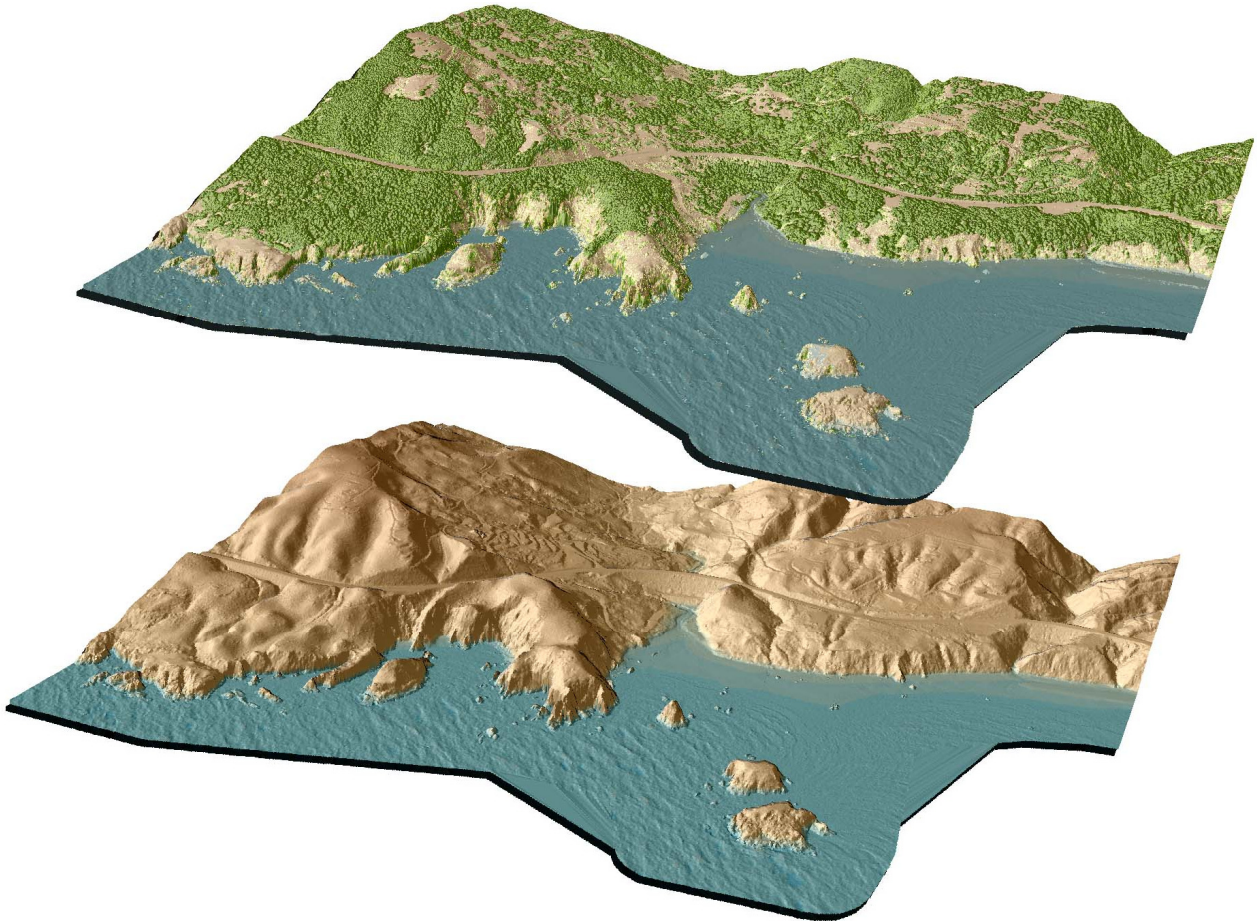


Figure 6.5. Oblique view to North over Chetco River and North Fork Chetco River (quad 42124-a2). Top image derived from LiDAR highest hits, bottom from bare earth LiDAR.

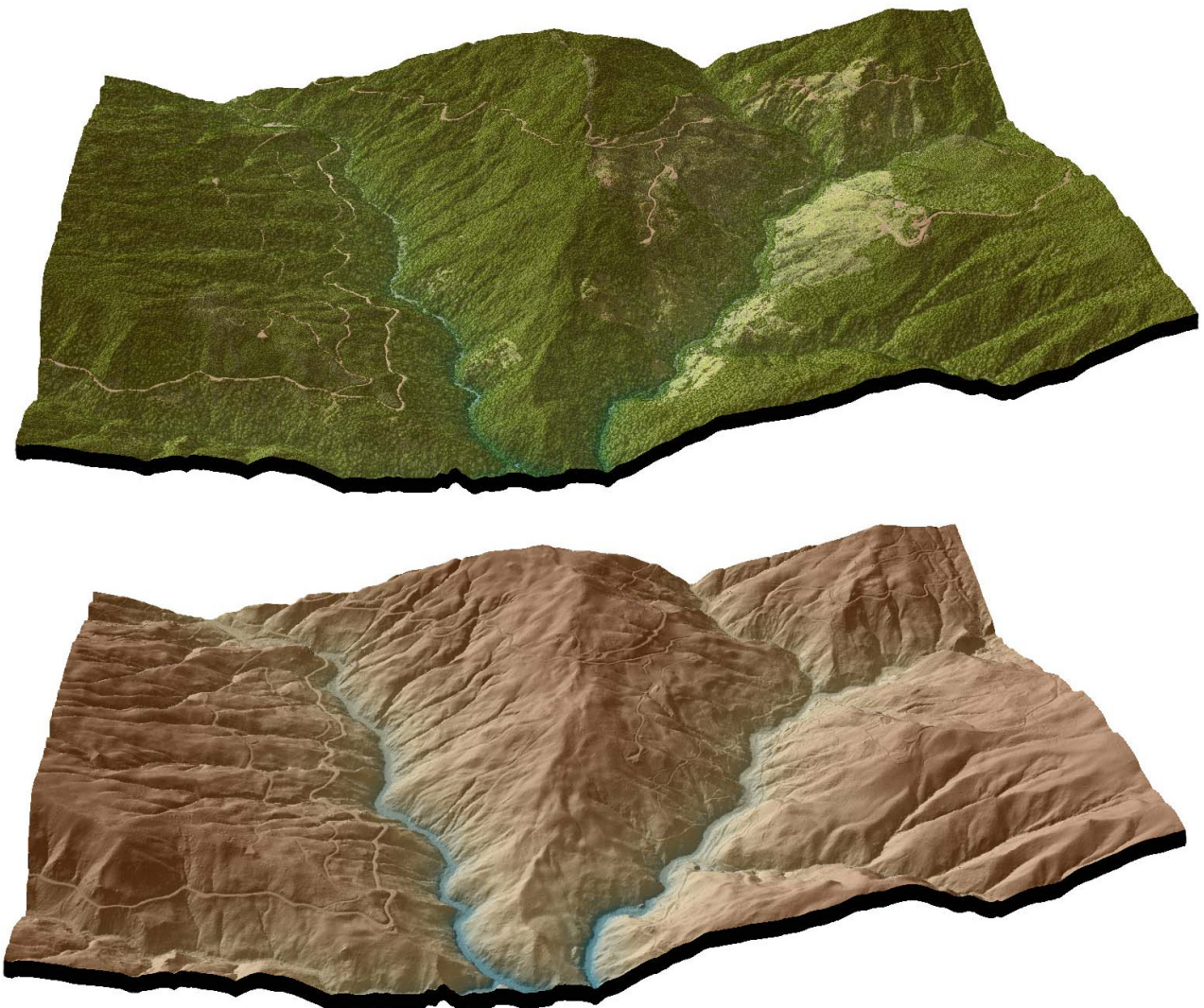


Figure 6.6. Chetco River upstream of confluence with Elk Creek (quad 42124-b2). Upper image derived from highest hit LiDAR, center image derived from bare earth LiDAR, lower image derived from NAIP orthophoto.



Figure 6.7. Whalehead and Coon Creek at terminus in ocean near Highway 101 (quad42124-b3). Top image derived from highest hit LiDAR, center image from bare earth LiDAR, lower image derived from NAIP orthophotos.



Figure 6.8. View of the Sixes River and Bea Creek confluence in delivery tile 42124g3. Top image derived from bare earth LiDAR, center image from highest hit LiDAR, and lower image derived from NAIP orthophotos.



Figure 6.9. View of the confluence of Sixes River and Edson Creek in delivery tile 42124g4. Top image derived from bare earth LiDAR, center image from highest hit LiDAR, and lower image derived from NAIP orthophotos.



7. Glossary

1-sigma (σ) Absolute Deviation: Value for which the data are within one standard deviation (approximately 68th percentile) of a normally distributed data set.

2-sigma (σ) Absolute Deviation: Value for which the data are within two standard deviations (approximately 95th percentile) of a normally distributed data set.

Root Mean Square Error (RMSE): A statistic used to approximate the difference between real-world points and the LiDAR points. It is calculated by squaring all the values, then taking the average of the squares and taking the square root of the average.

Pulse Rate (PR): The rate at which laser pulses are emitted from the sensor; typically measured as thousands of pulses per second (kHz).

Pulse Returns: For every laser emitted, the Leica ALS 50 Phase II system can record *up to four* wave forms reflected back to the sensor. Portions of the wave form that return earliest are the highest element in multi-tiered surfaces such as vegetation. Portions of the wave form that return last are the lowest element in multi-tiered surfaces.

Accuracy: The statistical comparison between known (surveyed) points and laser points. Typically measured as the standard deviation (sigma, σ) and root mean square error (RMSE).

Intensity Values: The peak power ratio of the laser return to the emitted laser. It is a function of surface reflectivity.

Data Density: A common measure of LiDAR resolution, measured as points per square meter.

Spot Spacing: Also a measure of LiDAR resolution, measured as the average distance between laser points.

Nadir: A single point or locus of points on the surface of the earth directly below a sensor as it progresses along its flight line.

Scan Angle: The angle from nadir to the edge of the scan, measured in degrees. Laser point accuracy typically decreases as scan angles increase.

Overlap: The area shared between flight lines, typically measured in percents; 100% overlap is essential to ensure complete coverage and reduce laser shadows.

DTM / DEM: These often-interchanged terms refer to models made from laser points. The digital elevation model (DEM) refers to all surfaces, including bare ground and vegetation, while the digital terrain model (DTM) refers only to those points classified as ground.

Real-Time Kinematic (RTK) Survey: GPS surveying is conducted with a GPS base station deployed over a known monument with a radio connection to a GPS rover. Both the base station and rover receive differential GPS data and the baseline correction is solved between the two. This type of ground survey is accurate to 1.5 cm or less.

8. Citations

Soininen, A. 2004. TerraScan User's Guide. Terrasolid.